STRUCTURAL, ELECTRONIC AND MAGNETIC PROPERTIES OF NIOBIUM NITRIDE POLYMORPHS FOR SUPERCONDUCTING APPLICATIONS: AN *AB-INITIO* STUDY

ISIAHO SOCLIFF LUDESHI

A THESIS SUBMITTED IN PARTIAL FULFILMENT OF THE REQUIREMENT FOR THE DEGREE OF MASTER OF SCIENCE IN PHYSICS OF MASINDE MULIRO UNIVERSITY OF SCIENCE AND TECHNOLOGY

MARCH, 2021

DECLARATION

This thesis is my original work prepared with no other than the indicated sources and support and has not been presented elsewhere for a degree or any other award.

Signature..................................... Date..

Isiaho Socliff Ludeshi

SPH/G/13/2015

CERTIFICATION

The undersigned certify that they have read and hereby recommend for acceptance of Masinde Muliro University of Science and Technology a research Thesis entiltled "**Structural, Electronic And Magnetic Properties Of Superconducting Niobium Nitride Polymorphs: An *Ab-Initio* Study**"

Signature.................................... Date................................

Dr Rapando B. Wakhu

Department of physics,

Masinde Muliro University of Science and Technology

Signature……………… Date………………………….

Dr Henry O. Otunga.

Department of Physics and materials science,

Maseno University

COPYRIGHT

DEDICATION

To my beloved mother, Margaret Khavulani, as an accomplishment of her desire for her children to excel in academics and reach the heights she never managed to get.

ACKNOWLEDGEMENT

First, I give thanks and praise to the ALMIGHTY GOD for the gift of life and the ability to work on this research to completion. Indeed he was faithful through the whole period of the study, in ups and downs he was my rock of refuge and my strength.

Special thanks go to my patient and knowledgeable supervisors Dr. Rapando Wakhu and Dr. Henry Odhiambo Otunga, who advised me, guided me on DFT, proof read and edited my work. I also acknowledge, first, my precious wife Brownice Kitisha for her patience and support during the period of the research, my father Fred Amudavi for financial support and lastly my fellow Msc course mates for their moral support.

Isiaho, S.L.

ABSTRACT

The quest for a hard superconducting material with engineering applications has been going on for some time. Among the hard superconducting materials is Niobium Nitride which superconducts at 17 K. Niobium nitride has excellent mechanical properties required for engineering applications and therefore has been the focus of research in the recent past. It has four structural polymorphs, that is, b1, b4, b81 and bh. Current research that has been done on this material has been skewed towards b1 and b81 leaving out the other two. In this work, Investigation basing on first principles on structural, electronic and magnetic properties for b1, b4, b81 and bh polymorphs was carried out. Comparison of the structural, electronic and magnetic propeties of the four polymorphs will help to assess the suitability of each polymorph for superconducting applications. In this work, calculations were performed using density functional formalism as implemented in the Quantum ESPRESSO computer code with the exchange-correlation functional in the local density approximation. Ultrasoft pseudopotentials was used to describe the electron-ion interactions. Initially, the optimized lattice parameters were obtained by fitting the total energy versus volume data to the Murnaghan equation of state. The structure was then relaxed until all the components of force on each atom was less than 10^{-3} Ry per a.u. The investigation reveals that b81 is the most stable with the least energy vs volume per formula unit. Phase transition is observed when pressure is exerted on the structures, with b81 transiting to b4 and b1 to bh. The four polymorphs have negative enthalpy indicating their possibility in synthesis. The density of states, band structures and charge density confirm that the polymorphs are metallic, good conductors, bonding is covalent and metallic. They are all found to be non-magnetic at zero K. Comparatively;bh stands out with the best qualities for superconductivity applications like making of superconducting wires, motors, magnetic recorders, Infra-red sensors and radio frequency superconducting accelerator cavities.

TABLE OF CONTENT

LIST OF TABLE

LIST OF FIGURES

ACCRONYMS AND ABREVIATIONS

b1	Rocksalt
b4	Wurtzite
b81	NiAs-type
bh	WC-type
DFT	Density Functional Theory
ESPRESSO	opEn Source Package for Research in Electronic Structure, Simulation and Optimization
FCC	Face Centred Cubic
FFT	Fast Fourier Transform
GGA	Generalized Gradient Approximation
LDA	Local Density Approximation
NbN	Niobium Nitride
T_c	Transition Temperature
XC	Exchange Correlation

CHAPTER ONE

INTRODUCTION

1.1 Background Information

Research on Superconducting hard materials (solid) like NbN has elicited interest from researchers in material science, solid-state physics and condensed matter physics both experimentally and theoretically. Niobium nitride polymorphs are some of nitrides materials that have been found to superconduct in solid state. Their excellent mechanical properties, that is, low compressibility, high hardness and high shear rigidity, makes them good candidates in electronic engineering, high pressure devices, motor systems, and carbon-nanotube junctions. They are also used as hard coating material, IR (infrared) sensor and in superconducting quantum interference devices. Coating material made from this compound (NbN) is characterized by high hardness especially in hexagonal phases (Holec *et al*., 2010).

Niobium nitride occurs in four polymorphs, that is; wurtzite (b4), WC-type (bh), rock salt (b1) and the NiAs-type (b81). The rock salt (b1) which has been widely studied among the four is cubic in structure (FCC); whereas, b4, bh and b81 have hexagonal trigonal P structures. Recent past theoretical calculations by first principle computational study shows that the Niobium Nitride hexagonal trigonal p structures exhibits high hardness and low total energy compared to the cubic one: rocksalt b1 (Zou *et al.,* 2016). The remarkable mechanical property of hardness of NbN hexagonal trigonal p superconductor makes them good candidates for engineering applications in motor system, carbon-nanotube and high pressure devices.

Superconductivity was discovered by Kammerlingh Onnes in 1911. It's a phenomenon where a conductor conducts dc current with zero resistance. The temperature at which a material starts to superconducts is referred to as transition temperature T_c and each material that superconducts has a unique T_c. Niobium nitride is a low T_c superconductor with the highest superconducting at 17K. The material has received more attention because it's a solid and ductile therefore, good for engineering applications

Computational techniques based on time dependent Schrödinger equation in DFT and as implemented in QUANTUM ESPRESSO code has been key in the recent times in predicting the properties of materials by calculation. The code uses the exchange correlation energy functionals like LDA, GGA etc in its calculation.

1.2 Statement of the Problem

Niobium nitride rock salt (b1) and NiAs-type b81 structures have been studied more extensively than the other two polymorphs: wurtzite (b4) and WC-type (bh). In the past studies researchers have done selective study of the four polymorphs. For instance, in one study on superconductivity; b81 is studied, whereas, in another b1, b81 and bh is discussed in light of thermodynamic property and another looks at b81, b1 and bh in light of structural, mechanical and electronic properties by first principles. Most of the above studies were pressure induced but this study is done at ambient pressure. Consequently, there has not been a comparative study of the four polymorphs in view of structural, electronic and magnetic properties in order to obtain a polymorph best suited for superconductivity applications. To utilize this hard superconducting material, it is essential to get the structural, electronic and magnetic properties of all the other polymorphs. In this research, a thorough study of the structural, electronic and magnetic properties of NbN is done for all the

polymorphs, the best suited polymorph for superconductivity applications determined. These physical properties are able to offerexceedingly detailed information for understanding other complex features of the material.

1.3 Objectives

1.3.1 The main objective

To investigate the structural, electronic and magnetic properties of Niobium Nitride polymorphs.

1.3.2 Specific objectives

   I.   To determine the structural properties of Niobium Nitride polymorphs.

  II.   To determine the electronic properties of Niobium Nitride polymorphs.

 III.   To determine the magnetic properties of Niobium Nitride polymorphs.

1.4 Justification

Niobium Nitride polymorphs were chosen for this research because of their good mechanical properties, that is; high incompressibility and they are ductile and therefore, can be drawn into wires. The four polymorphs of NbN were studied by looking at structural, electronic and magnetic properties consistently since other studies have tended to study one or two of the four polymorphs. In this research, *ab-initio* techniques are used to calculate the properties as implemented in QUANTUM ESPRESSO code using Local Density Approximation as an exchange correlation functional. Local density Approximation is chosen because it is easily available, cost effective and has good predictability factor in relation to the experimental values. The knowledge of structural, electronic and magnetic properties of the phases of NbN will be very important to researchers for further research in unraveling superconductivity and other properties of NbN.

1.5 Significance

Niobium nitride is currently the focus of materials research as a hard superconducting material. This study is important because the material has shown metallic properties and hence can be applied in making wires, motors and radio frequency superconducting accelerator cavities and infra-red sensors because it's ductile unlike other superconducting materials e.g cuprates that are brittle making them lack the applicability aspect.

1.6 Scope of the study

In this research, the focus will be on *ab-initio* calculation of structural, electronic and magnetic properties of NbN polymorphs.

CHAPTER TWO

LITERATURE REVIEW

2.1 Introduction

In this chapter, light will be shade on structural, electronic and magnetic properties of Niobium Nitride. In addition, its mechanical properties and superconductivity will also be discussed.

2.2 Structural properties of NbN

It's a 4d transition metal Nitride with four existing polymorphs; b1, b4, b81 and bh. The polymorph: b1 is referred to as rocksalt, b4 is Wurtzite, b81 is NiAs type and bh is WC-type. Among the four, b1 has a Face Centered Cubic structure (FCC) while b4, b81 and bh taking hexagonal trigonal P structure. The space group of b1 is F*m-3m*, b4 has space group of *P63mc*, b81 has space group of *P6₃/mmc* and lastly bh has space group of *P-6m2* (Jain *et al*., 2013). According to (Zhao *et al*., 2010) who investigated b1, b81 and bh with respect to their structural, mechanical and electronic properties using CASTEP code based on DFT and GGA-PBE exchange correlation functional, noted that the three had negative enthalpies at ambient pressure. The negative enthalpies show that the polymorphs can be synthesized easily by experiment. The calculated formation enthalpy for NbN was found to be larger by 22% in comparison to other theoretical values. In their analysis of the three polymorphs with reference to total energy against volume, showed WC-type to be more stable with least total energy per unit volume followed by NiAs-type and NaCl-type. The three polymorphs were also investigated by (Wang *et al*., 2011) using CASTEP code based on DFT and GGA-PBE exchange correlation functional, looking at pressure-induced structural transition and thermodynamic properties of

NbN and effect of metallic bonding on its hardness. They noted a pressure induced structural transition of NaCl-type to WC-type at 200.64Gpa at T=0K. Their calculated lattice parameters are as shown in the table 2.1 below.

Table 2.1: Optimized lattice parameters of NaCl, NiAs and WC by (Wang et al., 2011)

Structure	a (Å)	c (Å)
NaCl	4.408	
NiAs	2.975	5.549
WC	2.874	2.874

A plot of total energy versus volume per atom by (Ivashchenko *et al.*, 2010) confirmed that the hexagonal phases CW to be the most stable at various pressures. From the above two studies, b4 (Wurtzite) was left out. Moreover, in their calculations of lattice dynamic properties, they discovered soft phonon modes at the M points in NiAs structure indicating instability. This research is intents to do a thorough consistent comparative study of the four polymorphs of NbN.

2.3 Electronic properties of NbN

The electronic properties of materials, fundamentally depends on their Band structure graphs, Density of states (DOS) and charge density maps. These three depends on electronic valence configuration of Nb and N. In terms of orbitals Nb and N has a configuration of $4d^4$ $5s^1$ and $2s^2$ $2p^3$ respectively. The $2s$ of N do not take part in bonding because they are tightly bound by the nucleus; localized. But the d of Nb and the p of N participate in bonding and can result to any hybrid orbital with a coordination number higher than four (Holec *et al.*, 2010). The calculated electronic band structures of NaCl, CW and NiAs by (Ivashchenko *et al.*, 2010) exhibit three main bands. The lower energy band originating from N, $2s$ orbitals

followed by *d-p* band mostly associated by Nb *d* and N *p* states. The *d-p* states of NaCl does not split but CW and NiAs types splits into sub-bands related to the (Nb *d*-N *p*) σ and (Nb d- N p) π bonds. This therefore, means that the electronic property has a direct effect on the bonding. The superior mechanical property (hardness) of WC, NiAs and NaCl emanates from σ bonding states between the non-metal *p* orbitals and the metal *d* orbitals that intensely resists the shear strains (Zou *et al*., 2015). In reference to TDOS and PDOS as calculated by (Zou *et al*., 2016) it was noted that the NaCl and NiAs were metallic with a finite Dos at the Fermi level for NaCl. The pseudogap was also noted above/below the Fermi level indicating covalent and ionic bonds between Nb and N. The covalent like bonding is due to hybridization. From the resolved DOS WC structure shows strong hybridization both under zero pressure and high pressure (Wang *et al*., 2011). They also noted that the pseudo-gap separated the conduction band from the valence band.

2.4 Magnetic properties of NbN

Magnetism of a material is a result of the sum of spins and orbital magnetic moment of electrons. The mean electron spin per atom is magnetic moment which is used to characterize the magnetism of a material. In a case where the total electron spin per state is zero (there are two electrons per state having spin up and down and therefore couple) then the material is said to be diamagnetic. Where, the electrons don't pair (there is one electron per state) and all are oriented in the same direction the material has a magnetic moment of one, therefore, it's referred to us ferromagnetic. Anti-ferromagnetic is a material with electrons spins alternating in direction and its magnetic moment summing to zero (Sholl *et al*., 2009).

Diamagnetism has been observed in NbN by sweeping the field from zero to H_{c1}. It is noted that the temperature dependence of H_{c1} in both the bulk and micro-sized

crystal indicate that the H_{c1} for micro-sized crystal is greater and diverge to zero at $T_c = 8.7K$. This is because the micro-sized is more thinner than the bulk one therefore vortices cannot penetrate it easily in parallel magnetic fields (Wu *et al*., 2017). In addition, research has shown NbN NiAs-type to have metallic behaviour but doesn't have magnetism because their spin-up channel is symmetric to spin-down channel as shown by (Mora et al., 2018)

2.5 Mechanical properties

Mechanical properties are important especially when the material is being looked at for engineering application, where hardness and ductility are key. Niobium Nitride being part of the transition metal-nitrides has excellent mechanical properties; high hardness. For example the bh (WC-type) has low compressibility, high shear rigidity and high hardness (Zou *et al*., 2016), (Stampfl *et al*., 2001), (Bull *et al*., 2004), (Soignard*et al*., 2007), (Chen *et al*., 2005). The maximum hardness values are observed in hexagonal NbN polymorphs; b4, bh and b81 (Holec *et al*., 2010). Research that has been done on the 4d transition metal mononitrides from yttrium Nitride to Cadmium Nitride that is; (Yttrium, Zirconium, Niobium, Molybdenum, Technetium, Ruthenium, Rhodium, Palladium, Silver and Cadmium) on the Structural, electronic and mechanical properties with consideration of their WC-type (bh), rocksalt (b1) and NiAs-type (b81) structures using CASTEP code based on DFT and GGA-PBE exchange correlation functional. They discovered that the rock salt phase was stable in YN, ZrN, AgN and CdN, while NiAs phase was stable in MoN, TcN, RuN, RhN and PdN; whereas, WC-type was stable in NbN (Zhao *et al*., 2010). Focusing on Niobium Nitride alone where our interest is, it's clear that the Wurtzite (b4) is left out from Zhao and company research; where b1, b81 and bh had Bulk modulus of 312Gpa, 307Gpa and 316Gpa respectively. From the data, the

Bulk modulus was higher in bh than in b1 and b81. This therefore means that bh is harder than the other two polymorph of NbN, though all have high hardness. Other than looking at bulk moduli to predict the hardness of a material, the Debye temperature can also be used to predict the same. The higher the Debye temperature the harder the material (Zhao *et al*., 2010), the Debye temperature of b1, b81 and bh are 639K, 708K and 754K respectively. This implies that bh is the hardest of the three. The hardness is attributed to the insertion of Nitrogen in the metallic matrix. This results to formation of covalent bonds making the metal atoms less free to move and hence high hardness (Zou *et al*., 2015). It's clear from Zhao and company research that out of the four polymorphs of NbN only three were investigated. It is therefore, difficult to report with finality on all the four polymorphs of NbN

2.6 Superconductivity in NbN

Superconductivity is a phenomenon where a material conducts dc current without resistance below its T_c. It was discovered by Kammerlingh Onnes in 1911. Since then there has been unrelenting research in this field for a room temperature superconductor. For example, Hydrogen Sulphide has been discovered to superconduct at 203.5K under high pressure (Errea *et al*., 2015). Also, in recent times, Yttrium-based Hydrogen Clathrate is superconducting at room temperature, 303K at 400Gpa (Heil *et al*., 2019). Unfortunately the two cannot be applied in engineering because they lack the good mechanical properties (hardness) and ductility that NbN is well endowed with. Niobium nitride has receivedsubstantial consideration in the recent years due to its notable hardness, electronic and superconductivity in some of its polymorphs that has been researched on (Babu *et al*., 2019). Under the transition-metal nitrides that is; Zirconium Nitride, Hafnium Nitride and Niobium Nitride (rocksalt), it has been reported that Niobium nitride has

the highest transition temperature at 17.3K followed by Zirconium Nitride at 10K and Hafnium Nitride at 8.8K. When b1 and bh are compared on the basis of the T_c, b1 which is cubic is found to have higher T_c of 17.3K while bh has 11.6K. The difference in the T_c is alluded to the fact that, there exists a weak bonding in the Nb-N network for bh than in b1 (Zou *etal*., 2016). The high T_c in b1 is associated with the strong phonon-electron interaction in its lattice. According to (Zou *et al*., 2015), the transition temperature of b81 increase when subjected to pressure up to 20 Gpa. The pressure reduces the size DOS at the Fermi level reducing the electron-electron parameter which has a direct consequence on T_c. Since the NbN polymorphs have been proven to superconduct at low T_c they are applied in carbon nanotube junctions, Radio frequency superconducting accelerator cavities and hot electron photodetectors (Benvenuti*et al*., 1993), (Lindgren *et al*., 1998), (Kasumov*et al*., 1999). Therefore, the knowledge on the physical properties of NbN is important for a variety of scientific and technological and electronic engineering applications. It is also observed that superconductivity and mechanical property of a material largely depends on electronic property of the material (Meenaatci*et al*., 2013), (Jhi*et al*., 1999). Unfortunately research on superconductivity on NbN has been selective, with b1 and bh being studied more than the other two polymorphs. This research sought to determine the best material among the four polymorphs of NbN for application in superconductivity by studying the structural, electronic and magnetic properties of the four polymorphs.

In recent times, research has shown that T_c is highly related to the ground state energy from which energy, heat capacity and entropy are determined as shown by (Rapando *et al*., 2016) in their research using the diagonalized t-J Hamiltonian to work out the thermodynamic properties of high T_c superconductors. They noted that

the energy of the system reduced to zero as T=0K. This is very true, because superconductivity is a super-fluid state, where a buildup in temperature increases the energy of the system (Ulloa, 2019).

The intense research in cuprates is connected to their relatively high Tc. However, cuprates lack the applicability in engineering because they are brittle. This has caused a shift in research specifically for the search of a material with the right mechanical properties for application and superconducting at room temperature. Some of the prospects for applicability are lanthanum superhydride, ametallic hydrogen superconducting at 260K at a very high pressure (Somayazulu et al., 2019). Nevertheless, lanthanum superhydride is known to be soft malleable and ductile and oxidizes easily in air (Drozdov*et al*., 2019). Additionally, NbN has allured many researchers due to its excellent mechanical property: actually it is irreproachable when it comes to mechanical properties with high incompressibility compared to cuprates which have high T_c but brittle.

CHAPTER THREE

THEORETICAL BACKGROUND

3.0 Introduction

In this chapter Density Functional Theory is discussed with reference to many body systems, Hohenberg-Kohn theorem, Kohn-Sham equations, exchange correlation functionals, K-points, plane wave basis set and how to truncate a plane wave expansion and lastly pseudopotentials.

3.1 Many body systems

At the atomic level, it is quantum mechanics that provide the means to evaluate the ultimate properties of matter. Therefore, properties like optical, electrical and magnetic of a material can be found from the primary interactions between ions and electrons at the ground state.

The most intricate puzzle of condensed matter physics is the study of complex systems with many atoms and electrons and the various interaction between them.These systems can be illustrated using the time-independent and non-relativistic Schrödinger equation as shown below in equation (3.1).

$$\hat{H}(r;R)\psi(r;R) \equiv E\psi(r;R), \qquad\qquad 3.1$$

Where, $\hat{H}$ is the Hamiltonian of the system, ψ is the wavefunction $r \equiv \{r_i\}$ representing the electron coordinates, $R \equiv \{R_i\}$ representing the nuclei coordinates and E represents the total energy of the system and is also the eigenvalue of the Schrödinger equation. It is given as;

$$\hat{H}\left(\{r,P_i\};\{R,P_I\}\right) \equiv \sum_i \frac{P_i^2}{2m} + \sum_I \frac{P_I^2}{2M_I} + \sum_{i>j} \frac{e^2}{|r_i - r_j|} - \sum_{i,I} \frac{Z_I e^2}{|r_i - R_I|} + \sum_{I>J} \frac{Z_I Z_J}{|R_I - R_J|}$$

3.2

Where, m is the electron mass, P_i are the electron momenta, M_I is the nuclei mass with momentum P_I and the atomic number being Z_I (Mohammed, 2016). The Hamiltonian in equation (3.2) is summarised as;

$$\hat{H} \equiv \hat{T}_e + \hat{T}_n + \hat{V}_{ee} + \hat{V}_{en} + \hat{V}_{nn}$$

3.3

The first term on the right represents the electron kinetic energy operator; the second is the nuclei kinetic energy operator, the third is the nuclei potential operator acting on electrons while the fourth one is the electron-electron interaction operator and the last one is the nucleus-nucleus repulsion operator. The above results to large numbers of degrees of interactions that is (10^{23}); making the problem very intricate and it does not take care of double counting therefore necessitating Born-Oppenheimer approximations. It therefore requires an approximation to simplify the problem as proposed by (Kohn $et\ al.$, 1965) and (Hohenberg $et\ al.$, 1964). One of the approximations applied, is the Born-Oppenheimer approximation also known as adiabatic approximation. It considers the movement of electrons to be at a higher speed (quantum particles), and the ions being much heavier will seem to be at rest (classical particles) when compared to the electrons (Born $et\ al.$, 1927). Therefore, the electrons and the ions can be studied separately. The wave function of the system is expressed as the product of a function describing the electrons and that describing the ions.

$$\psi(r_i, R_I) = \phi(r_i, R_I) \times (R_I)$$

3.4

In consideration of equation 3.4, equation 3.2 takes the following form.

$$\left[\sum_i \frac{P_i^2}{2m} + \sum_I \frac{P_I^2}{2M_I} + \sum_{i>j} \frac{e^2}{|r_i - r_j|} - \sum_{i,I} \frac{Z_I e^2}{|r_i - R_I|} + \sum_{I>J} \frac{Z_I Z_J}{|R_I - R_J|} \right] \phi(r_i, R_I) = E_i(R_I)\phi(r_i, R_I)$$

$$3.5$$

In this case, the problem has been simplified into electrons and ion, however the 10^{23} degree of freedom remains a problem. From quantum mechanics, V_{nn} is treated as a constant, V_{en} as external potential but still V_{ee} is complex since the wavefunction of all the electrons depends on the coordinates of all electrons, therefore, they cannot be worked out singly. This complexity needs other tools to perform the calculation. One of these tools is Density Functional Theory.

3.2 Density Functional Theory (DFT)

Density functional theory is a ground state theory which emphasizes on the charge density as the relevant physical density (Martin, 2004). It has success in computing/calculating properties of many body systems in condensed matter. Currently there are many ab-initio codes that are applied in Density Functional Theory calculations; for example VASP, QUANTUM ESPRESSO, CASTE, ABINIT among others (Ahmed, 2015). In this research Quantum Espresso is applied which uses pseudopotentials and the plane-wave basis sets (Giannozzi *et al.*, 2009). The next is a brief review on development aspects of Density Functional Theory.

14

3.2.1 Kohn-Hohenberg Theorems

It is based on two theories that can be applied to interacting electron system subjected to external potential field $V^{ext}(r)$. Theorem 1 begins as follows;

Theorem I: In a case where electrons are interacting in an external potential field $V^{ext}(r)$ there is an agreement between a Hamiltonian with external potential $V^{ext}(r)$ and the ground state density $n_o(r)$ to an Eigen value which is the energy (Hohenberg *et al.*, 1964)

Proof I: The proof proceeds by *reductio da absurdum* (reduction to absurdity). If a many body system is subjected to two different external potential fields, V_1^{ext} and V_2^{ext} with Hamiltonian $\hat{H}_1, \hat{H}_2$ and ground state wavefunctions ψ_1, ψ_2 associated with each potential respectively it will give rise to two unique energies E_1, E_2. Further we assume that the wavefunctions have the same ground state density $n_o(r)$. Since the Hamiltonian $\hat{H}_1$ is related to the ground state wavefunction ψ_1 and with reference to the related variational principle, no wavefunction ψ can have an energy that is less than the energy of the wave function ψ_1 with respect to its Hamiltonian $\hat{H}_1$.

This gives;

$$E_1 = \langle \psi_1 | \hat{H}_1 | \psi_1 \rangle < \langle \psi_2 | \hat{H}_1 | \psi_2 \rangle \qquad 3.6$$

Assuming a non-degenerate ground state, the above inequality holds strictly. The last term on the right hand side of equation 3.6 can be expressed as equation 3.7 shown below; (Martin, 2004)

$$\langle\psi_2|\hat{H}_1|\psi_2\rangle = \langle\psi_2|\hat{H}_2|\psi_2\rangle + \langle\psi_2|\hat{H}_1 - \hat{H}_2|\psi_2\rangle, \qquad 3.7$$

$$= E_2 + \int d^3r\left[V_1^{ext}(r) - V_2^{ext}(r)\right]n_o(r)$$

Also; $\quad E_2 = \langle\psi_2|\hat{H}_2|\psi_2\rangle < \langle\psi_1|\hat{H}_1|\psi_1\rangle.$ \qquad 3.8

And, considering the second term in equation (3.6) we have;

$$\langle\psi_1|\hat{H}_2|\psi_1\rangle = \langle\psi_1|\hat{H}_1|\psi_1\rangle + \langle\psi_1|\hat{H}_2 - \hat{H}_1|\psi_1\rangle \qquad 3.9$$

$$= E_1 + \int d^3r\left[V_1^{ext}(r) - V_2^{ext}(r)\right]n_o(r),$$

Should be noted that the wavefunctions ψ_1 and ψ_2 in the equations above, results to the same ground state density $n_o(r)$. When equations 3.7 and 3.9 are added together we get;

$$E_1 + E_2 < E_2 + E_1 \qquad 3.10$$

The energies E_1 and E_2 represents the ground state energies corresponding to $\hat{H}_1$ and $\hat{H}_2$ respectively. Equation 3.10 is a contradiction. This is because there can never be two diffrent external potentials yielding the same groundstate electron density. Therefore, the ground state density corresponds one-to-one with Hamiltonian and the external potential field $V^{ext}(r)$ to a constant (Eberhard*et al.*, 2011).

Theorem II: The total energy $E[n]$ in terms of the density $n(r)$ can be expressed as a functional that is effective for any other external potential field $V^{ext}(r)$. Considering an external potential field $V^{ext}(r)$, the precise ground state energy of

the system will be the overall minimum value of this functional, and the density $n(r)$ that minimizes the functional is the correct ground state density $n_o(r)$ (Hohenberg *et al.*, 1964).

Proof II: As verified in the first theorem, (proof I), external potential with the Hamiltonian is distinctivelygoverned by the ground state density. The Hamiltonian also determines the ground state wavefunction. Therefore, the systems properties can uniquely be determined if $n(r)$ is specified. Subsequently, each property can be a functional of $n(r)$ and all summed up to total energy as shown below.

$$E[n] = T[n] + E^{\text{int}\,r}[n] + \int V^{ext}(r)n(r) \qquad 3.11$$

$$= F[n] + \int V^{ext}(r)n(r),$$

The first two terms on the right of the equal sign is the kinetic energy and the interaction energy between the electrons respectively. The two can be summarised into a functional $F[n]$ which has the kinetic and potential energies of interacting electron system. Subsequently if the kinetic and potential energies are a function of charge density, then $F[n]$ is a general functional (Martin, 2004). Tracking the argument in theorem I, then, if a system with ground state density $n_1(r)$ and a Hamiltonian $\hat{H}_1$ in the presence of an external potential field and a definite wave function ψ_1 will result to a ground state energy of;

$$E_1 = E(n_1) = \langle \psi_1 | \hat{H}_1 | \psi_1 \rangle \qquad 3.12a$$

If a different ground state density of $n(r)$ corresponding to different wavefunction ψ_2 is considered. Considering the variation principle, another density $n_2(r)$ will not basically give a higher energy

$$E_1 = E[n_1] = \langle \psi_1 | \hat{H}_1 | \psi_1 \rangle < \langle \psi_2 | \hat{H}_1 | \psi_2 \rangle = E^{n^{(2)}} \qquad 3.12b$$

Given the functional of the system $F[n]$ was known, therefore, by reducing the total energy with regard to the density function $n(r)$, we obtain the precise ground state energy and density.

Kohn-Hohenberg supported the being of a general functional $F[n]$ without decisively getting it, because $T[n]$ an approximation inherent in $F[n]$ has large errors, therefore the exact value of the functional is not known. This could have been the only loophole for doubts on the practicality of DFT; however, Kohn and Sham introduced another method in 1965 that eliminated the large errors in the functional (Martin, 2004) and (Kohn *et al.*, 1965)

3.2.2 Kohn-Sham equations

In their derivations, supposed that the density of interacting system is the same as that of non-interacting system; for the same system (Kohn *et al.*, 1965). Considering a system of N interacting electrons, its energy equation will be $\hat{H} = T + W + V$, where, the first term on the right is the kinetic energy term, the second is the interaction term with the external potential field and the last one is the electron-electron interaction. For the same kind of system but with non-interacting electrons N, its Hamiltonian will be; $\hat{H} = T^* + W^*$. The Kohn-Sham potential W^* represents the effective potential of a single electron. This effective potential field of a single

electron consists of the exchange correlation potential V_{xc}, external potential and the Hartree potential. The first potential (exchange correlation potential) is a function of the density of charge at the ground state that obeys the Pauli Exclusion Principle. Under K-S postulates, the density of the auxiliary system is given by the sum of the square of the orbitals.

$$n(r) = n(r)^* = \sum_{i}^{occup} |\phi_i(r)|^2 \qquad 3.13$$

ϕ_i is the single particle state of the non-interacting reference system. By Kohn-Sham method for interacting system, the ground state energy functional can be rewritten as,

$$E^{KS}[n] = T[n] + E^{ext}[n] + E^{Hatree}[n] + E^{XC}[n] \qquad 3.14$$

The first term on the right of the equal sign is the independent-particle kinetic energy, the second is the external energy due to the nuclei or any other external fields, the third one represents the coulomb interaction of the electron density interacting with the single electron and the last one is inherent of all the many body effects of the exchange and correlation energy. Kohn-Sham energy ($E_{KS}[n]$) is reduced with respect to the constant of orthonormality $\{\phi_i\}$. Applying chain rule on the functional derivatives, with all terms being functionals of the ground state density except T, which is a functional of the orbitals. We get;

$$\frac{\delta E_{tot}}{\delta \phi_i^*(r)} = \frac{\delta T}{\delta \phi_i^*(r)} + \left[\frac{\delta E_{ext}}{\delta n(r)} + \frac{\delta E_{Hartree}}{\delta n(r)} + \frac{\delta E_{xc}}{\delta n(r)} \right] \frac{\delta n(r)}{\delta \phi_i^*} = \varepsilon_i \phi_i \qquad 3.15$$

We can now write equation 3.12 as,

$$-\frac{1}{2}\nabla^2\phi_i(r)+\left[V^{ext}[n]+V^{Hartree}[n]+V^{XC}[n]\right]\phi_i(r)=\varepsilon_i\phi_i(r) \qquad 3.16$$

Equation 3.15 above is a mid-field equation of non-interacting system. Such kinds of system equations can be solved out iteratively.

3.3 Exchange and Correlation Functionals

Equations of Kohn-Sham are exact in principle; however, the Exchange-Correlation function is unknown and therefore approximated in practice. In most systems, the contribution of E^{XC} to the total energy is the smallest, yet it is 100% responsible for atomization energy (bonding between atoms/molecules). It has two parts, the exchange energy E^X and the correlation energy E^C. The E^X is guided by the Pauli Exclusion Principle which holds that two electrons with the same spin cannot have same energy. The exchange part is larger than the correlation part, and can be calculated exactly using Hartree-Fock method. The E^C part is due to the correlation and the exact value of this term is uncertain (Ahmed, 2015). Equation 3.16 V^{XC} and E^{XC} contain the exchange and correlation effects for a system of electrons. But the second one is the most important in the Kohn-Sham approach, on which Density Functional Theory calculations accuracy depends. The exchange correlation energy $E^{XC}[n]$ is dependent on the ground state density. The energy exchange correlation has several approximation discussed below.

3.3.1 Local Density Approximation (LDA)

It was the first simplest approximation of Exchange Correlation energy (E^{XC}) to be used, and was put forward by Kohn and Sham in 1965. In LDA, the XC-energy density of the inhomogeneous system with density $n(r)$ is locally approximated by the XC-energy density of an electron gas with density $n_o=n(r)$. It is therefore,

assumed that the electrons at the ground state behaved like a homogeneous gas. In LDA the E^{XC} is integrated over all space with the assumption that the exchange-correlation energy density is equivalent to that of a system with uniform electron gas at each point (Sholl, 2009) and (Kohn *etal*., 1965).

$$E_{xc}^{LDA}[(nr)] = \int \varepsilon_{xc}^{\text{homg}}(n(r))d^3r \qquad 3.17$$

Where $\varepsilon_{xc}^{\text{homg}}$ is the exchange correlation energy for an electron in a uniform electron gas. This exchange correlation energy can be determined accurately at any density $n(r)$, by applying the approximate version of the Green function Monte Carlo methods (Ceperley *et al*., 1980). Local Density Approximation is famous in underestimating the band gap by 40% (Perdew *et al*., 1981) and (Perdew, 1985) and predicts wrongly the magnetic property of iron (Perdew, 1985), (Sholl, 2004) and (Rinke *etal*., 2005).

3.3.2 Generalized Gradient Approximation (GGA)

It is a commonly used exchange-correlation energy approximation. It was proposed by Perdew and Wang in 1991. It uses the density and the density gradient in order to approximate the exchange correlation (Ahmed, 2015). GGA has evident improvement over LDA (Martin, 2004). It simplifies equation 2.15 of LDA, which is then defined as;

$$E_{xc}^{GGA}[n] = \int d^3r \varepsilon(n, \nabla n) \qquad 3.18$$

It is good in predicting molecular geometries, magnetic properties of 3D transitions metals and determination of ground state energies (Hellman *et al*., 2017). However, it has the following limitations; computationally it is expensive than LDA. Some of

the examples of GGA are; B88 by Burke, PW91 by Perdew and Wang and PBE by Perdew, Burke and Enzernof.

3.4 k-points

It is one of the key building blocks within DFT calculation. A summation over k-points is used to determine many quantities of condensed matter. The k-points allows the tracing and reconstruction of the wavefunction $\psi(r)$. They are used in sampling the first brillouin zone (1BZ), which defines the Wigner Seitz cell of the reciprocal lattice (Sholl *et al.*, 2009). The uniformly spaced Monkhorst-Pack k-point grid technique is a common approach used to sample 1BZ (Monkhost *et al.*, 1976). The Monkhorst-pack grids are in three dimension and denoted as; $N_{K_x} \times N_{K_y} \times N_{K_z}$, where, N_{K_i} specify the size of the grid in different directions. The denser the k-points size selected the heavier the computational cost; therefore, it's a computationally expensive parameter. According to computational principles k-points should be selected in infinite numbers, however, due to computational cost only finite grids are selected then a convergence is done to get the balance between the computational cost and accuracy (Mohammad, 2016).

3.5 Plane wave basis sets

In solving equation 3.16, the Kohn-sham equation, its wavefunction ψ is expanded in the basis set of;

$$\psi_i(r) = \sum_j^{N_b} C_{ij} f_j(r),$$

3.19a

Where the first term under the summation C is the weight of the plane wave, the second term $f(r)$ is the basis function and the size of the basis is N_b. Many basis

functions exist and the following are the common examples; plane waves, localized set. The localized set is made of the Gaussian and mixed basis sets. The Plane waves basis set allows easy calculations of derivatives and integrals. They also don't depend on atomic positions and involve the Fast Fourier Transform (FFT) that can rapidly transform the plane waves from r-space to k-space and back. This is important when dealing with the Bloch wavefunctions for periodic system like solids. These are the reasons why plane waves are commonly used. The Bloch wave functions for a periodic system is as shown below.

$$\psi_K(r) = e^{ik.r} u_k(r) \qquad\qquad 3.19b$$

The amplitude factor of the wave with its' periodicity as $u_k(r)$. Its' Fourier transform is;

$$u_k(r) = \frac{1}{\Omega} \sum_G C_k, Ge^{iG.r} \qquad\qquad 3.20$$

The reciprocal lattice vector is G and the lattice volume is Ω. Substituting equation 3.20 into equation 3.19b, gives as the Bloch state of the plane wave expansion in a periodic system as shown below in equation 3.21.

$$\psi_K(r) = \frac{1}{\Omega} \sum_G C_K, Ge^{i(K+G).r} \qquad\qquad 3.21$$

3.5.1 How to truncate the plane wave expansion/cut-off energy (E-cut)

The function of the lattice periodicity is expanded in forms of plane waves that include reciprocal vectors G. But, in equation 3.21 the summation over G is very long and requires a long time to compute. This requires the determination of correct point to end the summation. Therefore, in practice, the truncation takes place at the value $|K+G|$. This value is expressed in energy units and it follows the condition

23

$\dfrac{\hbar^2 |K+G|^2}{2m} \le E_{cut}$. Cut-off energy in DFT calculations is a significant factor; therefore, picking the right converged cut-off energy value with respect to total energy for a given system is of great importance. Therefore the computational effort is reduced without affecting accuracy and prevents artifact of unit cell orientation on numerical results (Mohammad, 2016).

3.5.2 Pseudopotentials

The coulombic potential of the nuclei on the electrons in a system leads to computational hitches, particularly when the plane waves are used as basis set in expanding the wavefunction. The solution to this problem is separating the atom into core and valence electrons. Wavefunctions of core electrons are sharply peaked close to the nucleus while the wavefunctions of the valence electrons wiggles more due to their orthogonality to the core. Thus, they normally need higher Fourier components that is, higher cut-off energy. This hitch is overcome by the use of pseudopotential approximation. In pseudopotantial approximation, the atoms that make-up the chemical system are altered through elimination of the core electrons degrees of freedom and the valance electrons are then described by the pseudo-wavefunctions, that are fairly smooth in comparison to the real wavefunctions in the core region, (Troullier *et al*., 1991). Pseudopotential methods are advantageous because they use the plane wave basis set unlike the full potential methods (Phillips *et al*., 1959). The pseudo-wavefunctions being smooth with the strongly related numbers of orbitals considerably reduce the computational cost (Hutter *et al*., 2010). The most common pseudopotentials are, Ultra Soft, Projected Augmented Wave (PAW), and Norm-conserving types of pseudopotentials (Kresse *et al*., 1999). In this

study Ultra-soft pseudopotentials is used because it requires substantially low cut-off energy than alternatives.

CHAPTER FOUR

COMPUTATIONAL METHODS

4.0 Introduction

In this work, the structural, electronic and magnetic properties of NbN polymorphs has been calculated using density functional theory as implemented in the QUANTUM ESPRESSO computer code (Giannozi *et al*., 2009). It uses the pseudopotential approach which allows it to calculate many material properties. It is multi-purpose, multi-platform software for *ab-initio* calculation of periodic and non-periodic condensed matter. The Local Density Approximation as parameterized by Perdew and Zunger (Perdew *et al*., 1981) was considered for the exchange-correlation energy functional due to its low cost and availability. The ion-electron interactions are described using Ultra-soft pseudopotentials. To sample the brillouin zone, k-mesh point densities were used as per the Monkhorst-Pack scheme (Monkhorst *et al*., 1976).

To calculate the ground state density, Quantum ESPRESSO uses the self-iterative cycle to solve the Kohn-Sham functional in equation 3.16. The Kohn-Sham equations are solved interactively to self-consistency. Fig:4.0 illustrates the scheme of the self-consistent calculation of the Kohn-sham equations.

V_{nuc}

$n_{(r)}$

$V_{nuc}[n]$ $V_{XC}[n]$

$$V_{eff}(r) = V_{nuc}(r) + V_H(r) + V_{XC}(r)$$

$$H\psi_i(r) = \left[-\frac{1}{2}\nabla^2 + V_{eff}(r)\right]\psi_i(r) = \varepsilon_i\psi_i(r)$$

$$n(r) = \sum_i |\psi_i(r)|^2$$
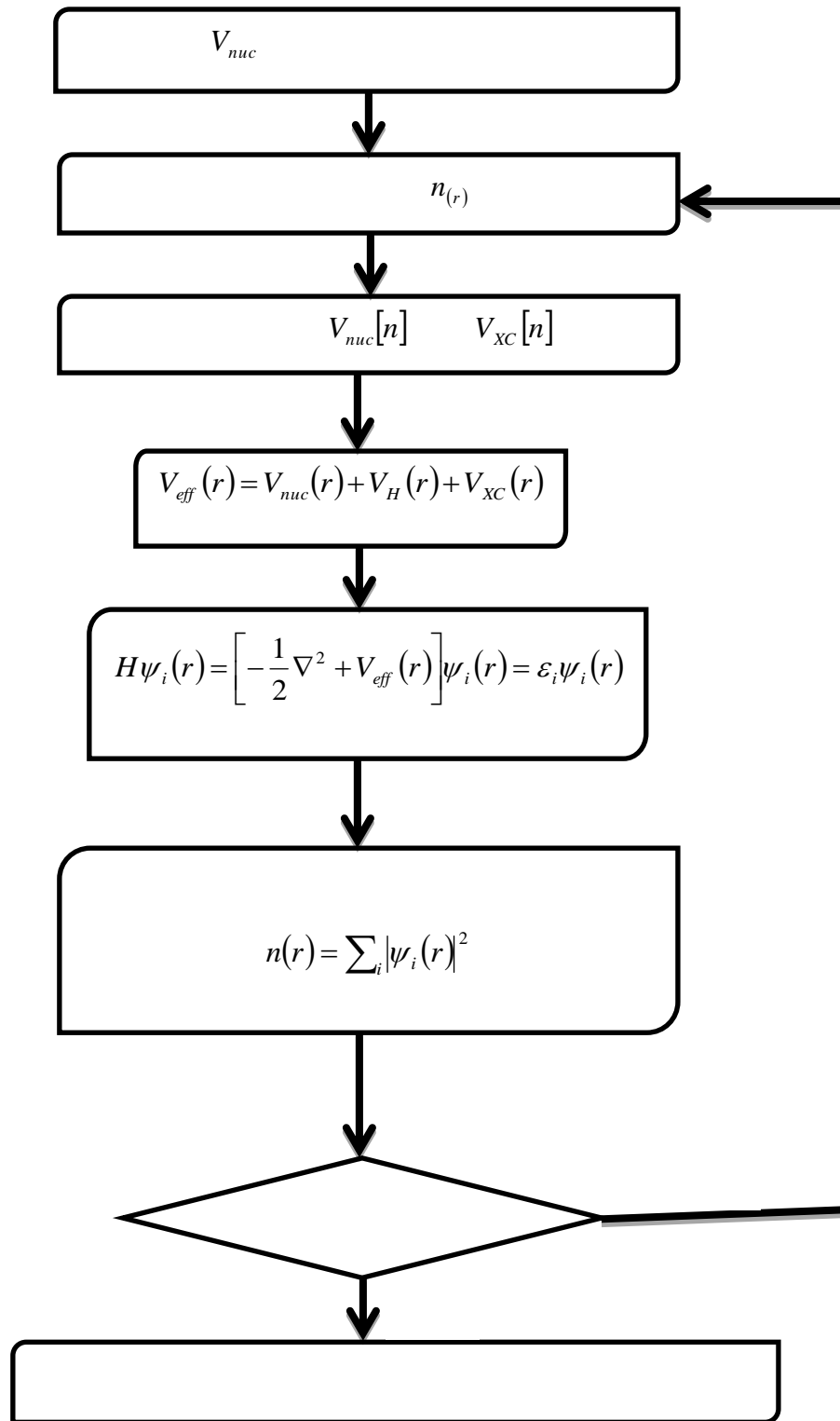
Fig: 4.0 Flow of calculations in the self-consistent solutions of Kohn-Sham equations (Woods *et al.*, 2019)

4.1 Optimization of k-points and Plane Wave Energy cut-off.

4.1.1 k-points

The k-mesh points were optimized using the experimental lattice parameters shown in Table: 4.1 of NbN polymorphs and setting the kinetic cut-offs energy was at 70Ry for all the polymorphs then generated by the monk-horst pack scheme. For NbN polymorphs; b1, the k-mesh is integrated over unshifted mesh to a dense one of ($10\times 10 \times 10$), while bh and b81 the k-mesh is integrated over shifted to a dense one of ($10 \times 10 \times 10$) and b4 the mesh is integrated from unshifted to a dense one of ($7 \times 7 \times 7$). The dense mesh was required since transition metals are known to require large k-points grids (Sholl *et al*., 2009). For each polymorph, the values of total energy and k-points are plotted and the stable k-points are noted at unshifted ($9\times9\times9$) for b1, shifted ($9 \times 9 \times 8$) and ($9 \times 9 \times 6$) for bh and b81 respectively and unshifted ($5 \times 5 \times 3$) for b4 as shown in the figures 6.2a-6.2d in the appendices of Total Energy Vs k-points where the graph becomes monotonic. When calculating k-points the atoms are fixed to set a fixed k-grid. The optimized k-points were used for all calculation to ensure accuracy in this research.

Table 4.1: Experimental lattice parameters

NbN phase	*a* (Ry)	*c* (Ry)	References
b1	8.2751		Wang *et al*., 2010
b4	6.0471	3.118	Holec *et al*., 2010
b81	5.609	10.486	Ogot *et al*., 1995
bh	5.533	5.272	Ogot *et al*., 1995

4.1.2 Plane wave energy cut-off optimization

The converged k-points for b1, bh, b81 and b4 are used to calculate the kinetic cut-off energy for each polymorph. Kinetic cut-off energy of 70Ry was used for all the polymorphs. Charge density cut-off energy of 560Ry (energy cut-off x 8) was used for all polymorphs. The optimized values of kinetic cut-off energy and k-points are used to calculate the bulk properties of the polymorphs of NbN.

The E-cut for b1, b4, b81 and bh was set at 70 Ry as from graphs 6.3a-6.3d in the appendices, while the charge density cut-off was set at 560Ry.

The k-points and E-cut are key in optimization of structures, for they set the boundary within which the structure exists. The DOS is also arrived at by integrating the k-point along the high symmetry points to get the electronic property. This DOS can also be symmetrically be optimized to get spin up and spin down that determines the magnetic property.

4.2 The Structural properties of Niobium Nitride polymorphs.

The structural optimization was done using the converged k-points for all the four polymorphs of NbN and there optimized kinetic energy cut-off and charge density cut-off of 70Ry and 560Ry in that oder. The lattice parameters are gotten by fitting the total energy versus volume data to the Murnaghan equation of state. The volume is determined through the grep! command whose output file is fitted on the Murnaghan equation of state (Tyuterev *et al*., 2006) and (Murnaghan, 1944).

$$E_b(V) = \frac{B_o V}{B_o'(B_o' - 1)} \left[B_o' \left(1 - \frac{V_o}{V} \right) + \left(\frac{V_o}{V} \right)^{B_o'} - 1 \right] + C_b \qquad 4.1$$

Where the integration constant $C_b = -\dfrac{B_o V_o}{B'_o - 1}$, V_o is the theoretical equilibrium unit cell volume, B_o is isothermal bulk modulus and B'_o is the derivative of isothermal bulk modulus. These correct parameters are attuned to make $E_b(V)$ coincide with $E_{calc}(V)$

The atomic positions were then optimized by performing a relax calculation such that the components of force on each atom are less than 10^{-3} Ry. The lattice constants are calculated by fitting the Total energy and optimized volume on the murnaghan equation of state. The structures are optimized until the energy and the forces are well converged. The optimized structures are as shown in fig 4.21.

The output file also comprises of formation enthalpy and pressure which are plotted and discussed in chapter 5 Fig: 5.12 and 5.13
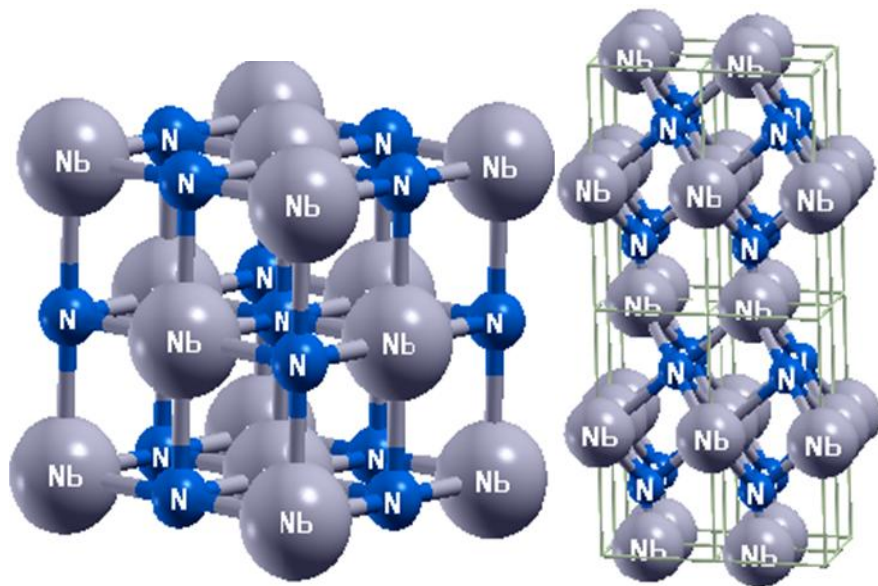
b1   b4
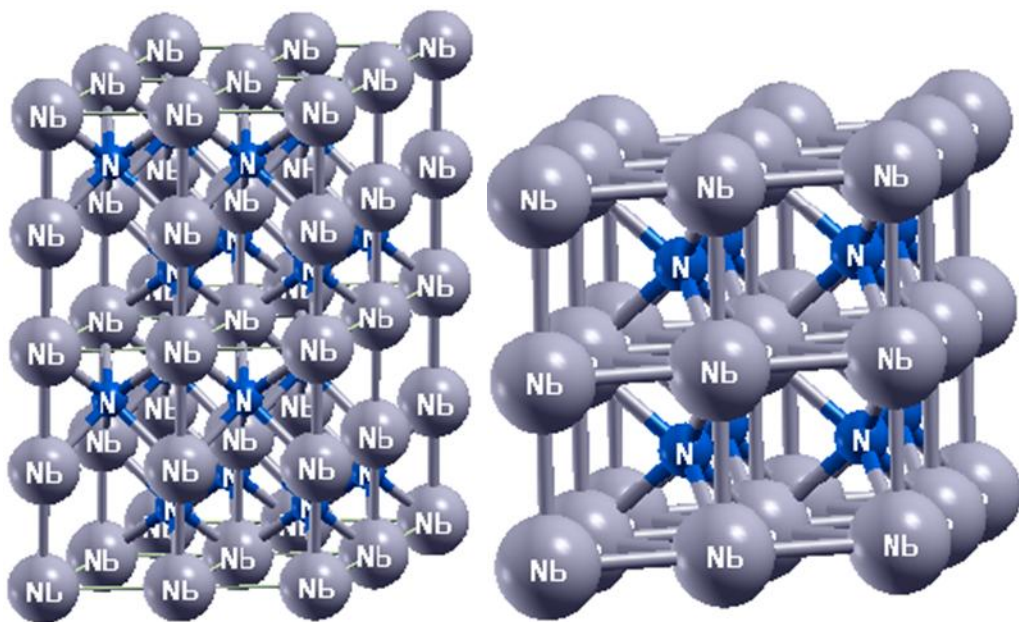
b81   bh

Fig: 4.21 b1 unit cell, b4 2×2×2 supercell, b81 2×2×2 supercell and bh 2×2×2 supercell. Nb atoms are grey and N atoms are blue in colour.

4.3 Determination of the electronic properties of Niobium Nitride polymorphs.

Computation of the electronic properties is based on electronic density of states, band structure and the charge density of the material under research.

Band Structures

The electronic band structures was calculated by integrating the k-points along a high symmetry path of ΓXWLΓK for b1 and ΓAHKΓMLH for b4, b81 and bh respectively in the k-space as shown in fig: 4.3a and 4.3b
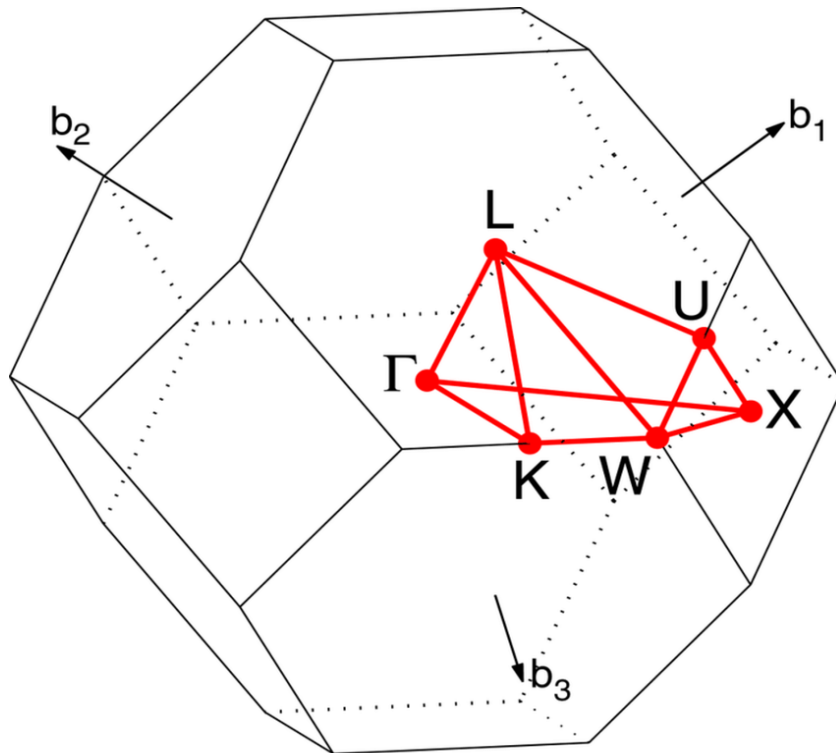
Fig: 4.3a High symmetry points used for b1 FCC structure in this study

(setyawan*etal*., 2010)
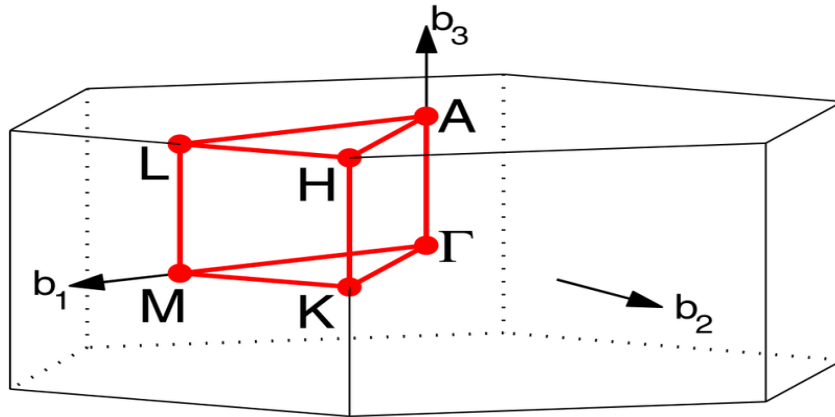
HEX path: Γ-M-K-Γ-A-L-H-A|L-M|K-H

[Setyawan & Curtarolo, DOI: 10.1016/j.commatsci.2010.05.010]

Fig: 4.3b High symmetry points used for b4, b81 and bh Hexagonal structure in this study (setyawan*et al*., 2010).

The results of calculation of band structures were plotted as shown in fig: 5.21a-5.21d.

Density of states

The DOS is one of the basic quantities used to describe the electronic state of a material. In DFT plane wave calculations, the DOS is expressed in wave functions of the form exp(*ik.r*). The electrons associated with plane waves of this form have energy $= \frac{(hk)^2}{2m}$. Therefore, the electronic DOS can be resolved by integrating the resulting electronic density in the k-space. That is the k-grid sampled for b1, b4, b81 and bh of NbN polymorphs. The DOS helps to determine the concentration of electrons at the Fermi level and the size of the gap between valence band and conduction band if any. The band gap between the valence band and the conduction band is used to classify the material whether it is a semi-conductor or an insulator.

Charge Density

The calculation of charge density proceeded by making a self-consistent calculation file for each polymorph (NbN.scf.in). Then a post processing program pp.x was run in the form of (input=NbN.pp_rho.in, output= NbN.pp_rho.out) in order to extract a 2D cut of charge density. To plot the charge density maps, plotrho.x program was invoked (with input file as NbN.plotrho.in and output file as NbN.plotrho.out) to give a postscript file (NbN.rho.ps).

4.4 Determination of the magnetic properties of Niobium Nitride.

Magnetic property like Meissner effect is also an important factor in determining superconductivity of a material. Meissner effect is a magnetic characteristic where a superconducting material repulses magnetic flux from its interior when T_c is reached or below T_c. This means the material below T_c exhibit perfect diamagnetism. Also superconductivity can be abolished by applying magnetic field on a superconductor above the critical field value H_c. It therefore means that the transition to superconductivity can be indicated by the critical field other than the transition temperature. To determine diamagnetism Spin polarized DFT are performed using plane-wave basis set implemented in the quantum ESPRESSO package with LDA being the exchange correlation functional and ultra-soft pseudopotential for the four polymorphs NbN. The total absolute magnetization would be achieved using self-consistent functional calculation as the integral of magnetization in the cell and the integral of the absolute value of the magnetization. The polarization electron spin at the Fermi level is defined by the following expression;

$$P = \frac{\eta \uparrow (E_F) - \eta \downarrow (E_F)}{\eta \uparrow (E_F) + \eta \downarrow (E_F)},$$

<div align="right">4.2</div>

Where $\eta\uparrow(E_F)$ and $\eta\downarrow(E_F)$ are the spin dependent densities of states at Fermi level for the majority and minority spins in that order. In this study, the calculation of magnetic property is done at zero K.

5.0 Introduction

In this chapter, results collected are reported and discussed comparatively across the four polymorphs. The generated structural properties are discussed followed by the evaluated electronic properties and lastly the magnetic properties of Niobium Nitride polymorphs.

5.1 The Obtained Structural properties of Niobium Nitride polymorphs for superconductivity applications.

5.1.1 Optimized Lattice Parameters

The structural properties help in understanding the compound solid properties from the microscopic point of view. The optimized lattice parameters and cell volume for the four polymorphs are listed in table 5.1 shown below. For b1 lattice parameter a is less than the experimental value, while the theoretical value calculated by Zhao is greater. This can be alluded to the exchange correlation functional used. Zhao and company used GGA-PBE whereas; in this research LDA was used. It therefore proofs the fact that LDA underestimates the volume while GGA over estimates the volume.

In b4, there is a large deviation in lattice parameter a and c. for instance, lattice parameter a by the theoretical work of Holec and company using GGA-PBE as exchange correlation functional and the present work calculated using LDA overestimate a and underestimates c. The disparity is connected to the cut-off energy set: that is, 952eV for the present work and 450eV by Holec and company.

For b81, the deviation from experimental value is below plus or minus 4%. It is clear from the table that there is a close agreement with the other theoretical and experimental values. Lastly in bh the deviation in lattice parameters is below +5.01% and above -1.61%.

The lattice parameters are used to determine the volume of the structures. The volume also determines the charge density which has a direct consequence on electronic and magnetic property.

Table 5.1: Optimized lattice parameters

	b1 (NaCl)			
Property	**Present work**	**Experimental value**	**theory**	**Deviation %**
a (a.u)	8.2596	8.2751	8.3337	-0.19
Volume (a.u)^3	140.8695			
References		(Chen *et al*., 2005)	(Zhao et al., 2010)	

	b4 (Wurtzite)			
a(a.u)	6.226	6.047	6.198	+2.96
c(a.u)	10.209	18.855	17.683	-45.85
c/a	1.6397	3.118	2.853	-47.41
Volume (a.u)^3	342.7065			
References		(Holec *et al*., 2010)	(Holec *et al*., 2010)	

	b81 (NiAs)			
a(a.u)	5.823	5.609	5.580	+3.81
c(a.u)	10.517	10.486	10.376	+0.295
c/a	1.8061	1.869	1.8595	-3.37
Volume (a.u)^3	308.8081		279.7879	
References		(Ogut*et al*., 1995)	(Wang *et al*., 2011)	

	bh (WC-type)			
a(a.u)	5.444	5.533	5.575	-1.61
c(a.u)	5.448	5.272	5.424	+3.33
c/a	1.0007	0.953	0.9729	+5.01
Volume (a.u)^3	139.8263		145.9914	
References		(Ogut*et al*., 1995)	(Wang *et al*., 2011	

5.1.2 Total energy vs Volume per unit formula

Before plotting, the Total Energy and corresponding volumes are divided by the number of atom per unit cell to get the Total energy and volume per formula unit. For instance, b1 and bh has two atoms per unit cell while b81 and b4 have four

atoms per unit cell. The point of concern is the turning points of each graph, the lower the turning point, the lower the energy per volume per unit formula. Therefore, according to Fig:5.1.1, b81 was found to be more stable than the other three polymorphs, since it had the lowest total energy per formula unit according to the graph of total energy versus volume as shown in fig. 5.11 below. It is also clear; wurtzite b4 (hexagonal) has the highest energy volume formula unit. The graph also, showed that the energies of the rocksalt b1 (cubic) and WC-type, Bh (hexagonal) were closer to that of NiAs-type, b81 (hexagonal), as confirmed by (Wang *et al*., 2011). The polymorph with the lowest energy per volume per unit formula is the most stable structure.
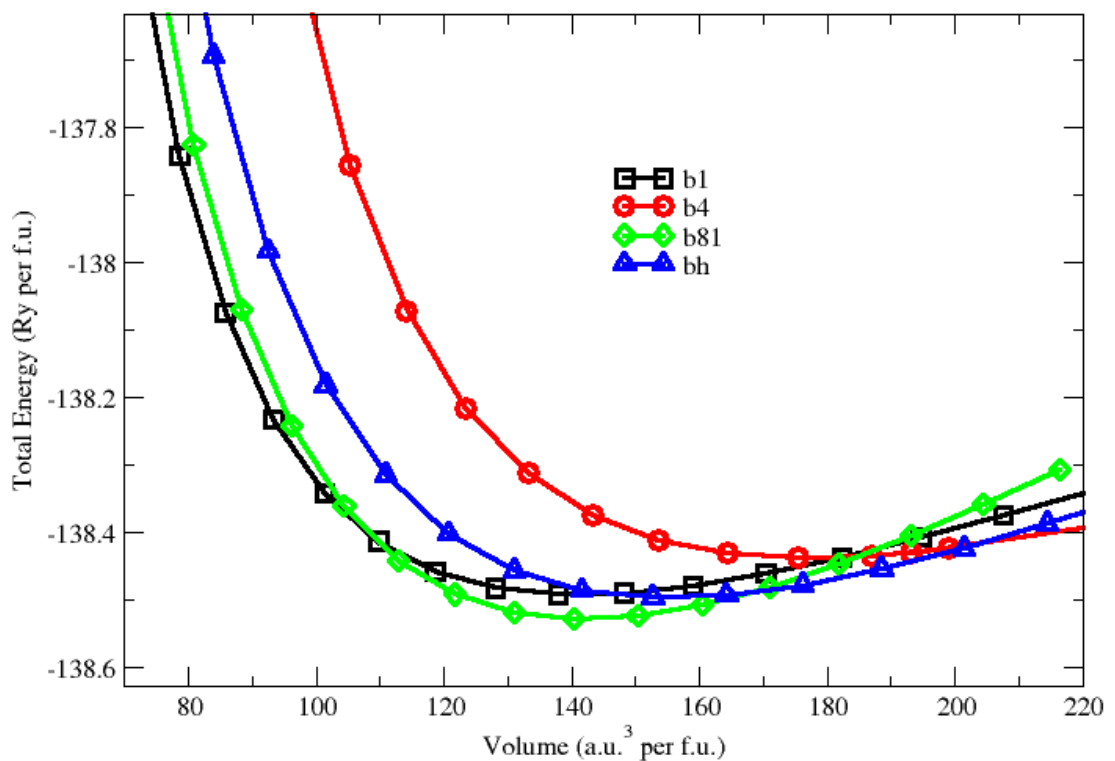
Fig: 5.11 Total Energy vs Volume per formula unit for NbN polymorphs

Superconductivity is a low energy phenomenon. Therefore it would probably occur in polymorphs with low energy per volume per unit formula

39

5.1.3 Variation of Enthalpy of formation as a function of Pressure

The plot of enthalpy of formation versus pressure helps to indicate the transition of structures from one form to the other within the family. It also helps to show the pressure at which the structures can occur.

According to this research, Pressure-induced structural phase transition from bh to b1 occurred at -1.51961GPa and from b81 to b4 it took place at -21.7402Gpa using QUANTUM ESPRESSO code and Local Density Approximation (LDA) exchange correlation functional as shown in Fig:5.12. However, (Wang *et al*., 2011) who investigated pressure induced structural transition of NbN, specifically looking at b1, b81 and bh, indicated a phase transition between b1 to bh at 200.64Gpa using Cambridge Serial Total Energy Package (CASTEP) with Perdew-Berke-Ernzerhof form of Generalized Gradient Approximation (GGA) as the exchange correlation functional. The difference in the pressure of the structural transition from b1 to bh could be due to two reasons. First and foremost, in this research, cut-off energy was set at 70Ry (952.40eV), whereas, (Wang *et al*., 2011) had set their cut-off energy at 450eV which is less than a half of the value in this research. The cut-off energy is a basic quantity that is important in determining ground state properties and it has a direct impact on the outcome of pressure induced structural transition. According to (Syrivasta*et al*., 2011) the large deviation is due to the type of interactions taken into consideration during calculation. Another factor is the exchange correlation functional that was used. For this research, LDA was employed which assumes uniform electron density in the ground state. On the other side, GGA was used as an exchange correlation functional and works with slowly varying electron density at the ground state, thus the difference in the outcome of transition pressure.
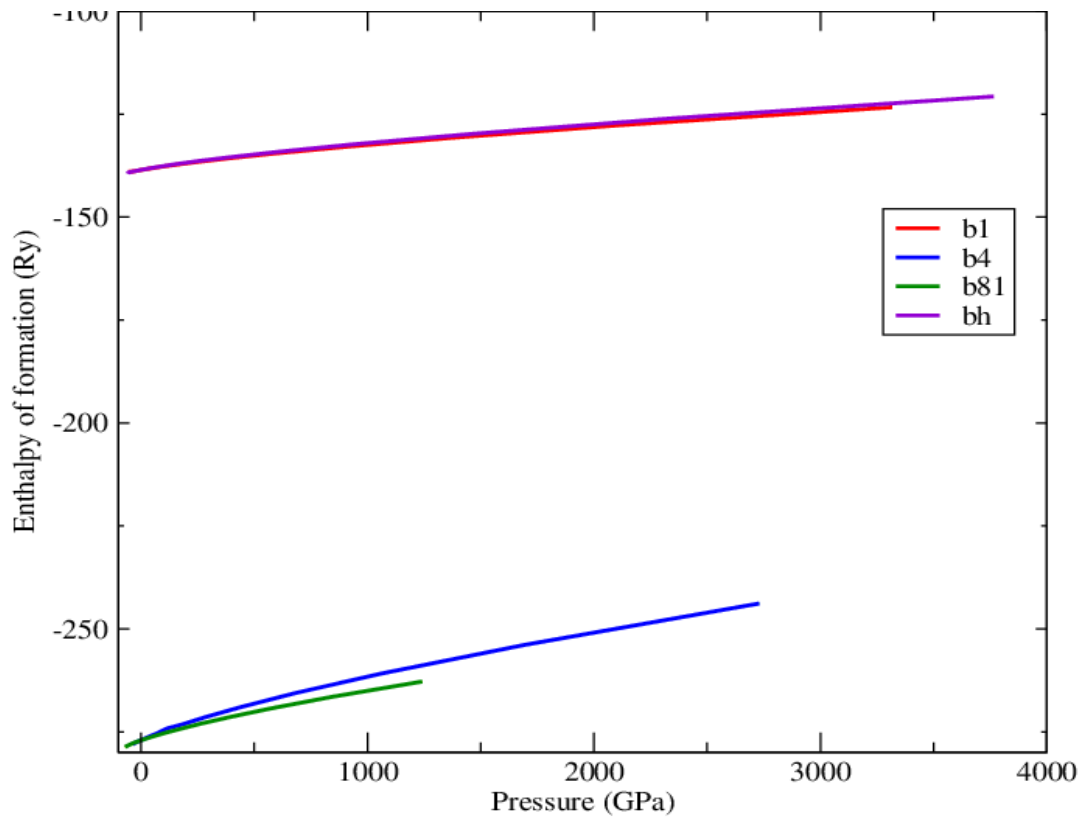
Fig: 5.12 Enthalpy as a function of Pressure at T=0K.

The four polymorphs are observed to have negative enthalpy with b81 having the least followed b4, b1 and bh at -278.908 Ry, -278.277 Ry, -139.419 Ry and -139.244 Ry respectively. Therefore, energetically, b81 is more stable followed by b4, b1 and bh. Since the enthalpies of the four are negative, it means they can be synthesized at ambient conditions.

According to (Rapando *et al*., 2016), superconductivity is a low energy phenomenon and will probably manifest in structures that have low enthalpy. In addition, (Rapando *et al*., 2014) alluded that total ground state energy (Enthalpy) of a superconducting system is directly related to the T_c of the system. Therefore, the lower the ground state energy the smaller the energy gap which is a function of

superconductivity. They formulated an equation that could give energy of the system at any particular temperature; that is,

$$E = (J + 4t)e^{-\left(\frac{(J+4t)}{100KT}\right)},$$

Where, J is the spin transfer integral, t is the hoping integral, K is the Boltzmann's constant and T is the temperature of the system. Also, as shown by the Helmholtz free energy per unit volume equation F= U- TS. Where F is the Helmholtz free energy, U is the total internal energy (enthalpy) including interaction of charges, coulombic attraction and repulsion and magnetic interactions that is, magnetic coupling and spin pairing. The two equations correspond to what is referred to as bonding enthalpy. T is the temperature of the system while S is the entropy of the system (Marouchkine, 2004). Therefore it's clear that a superconducting system with the lowest enthalpy will give the lowest Helmholtz free energy that is required for superconductivity. According to the graphs of enthalpy as a function of pressure shown in fig: 5.12 and 5.13, b81 has the lowest enthalpy followed by b4, b1 and bh. It follows that, b81 has the lowest enthalpy therefore, the best candidate for superconductivity.

5.2 Determined Electronic Properties of Niobium Nitride polymorphs.

5.2.1 Evaluated Band structures and Density of States

Figure 5.21a-5.21d below clearly shows the calculated density of states and band structures for b1, b4, b81 and bh. The four graphs of DOS confirm the separation of N-*s* states from the other states. For b1, the N-s states lie at approximately (-15 to -18) eV, while, b4 is at (-15 to -16) eV, b81 (-14 to -16) eV and bh is at (-14 to -16) eV, with their width differing approximately by 1.0eV. The peak of N-s state in b4 is

highest compared to the other three polymorphs. These states (N-s) do not participate in bonding because they are strongly held by the core of the atom. The other states, mainly, N-*p* and Nb-*d* occupy (-9 to 5) eV for b1, (-5 to -7) eV and (- 2 to 11) eV for b4, (-9 to 12) eV for b81 and (-9 to 12) eV for bh. The Fermi level for b1, b4, b81 and bh is 20.85 eV, 16.33 eV, 18.03 eV and 19.97eV respectively as generated by system. There is a sharp depression (pseudogap) above the Fermi level of b4 and below b81, in bh the pseudogap lies at the Fermi level whereas, in b1 there is no pseudogap. In all the DOS graphs the densities at the Fermi-level is non-zero. This means, the polymorphs are all metals and good conductors of electric current due to the free electrons in the valence band. Finally, it is worth noting that the DOS at the Fermi level is highest in b4 followed by b81, b1 then lastly bh.
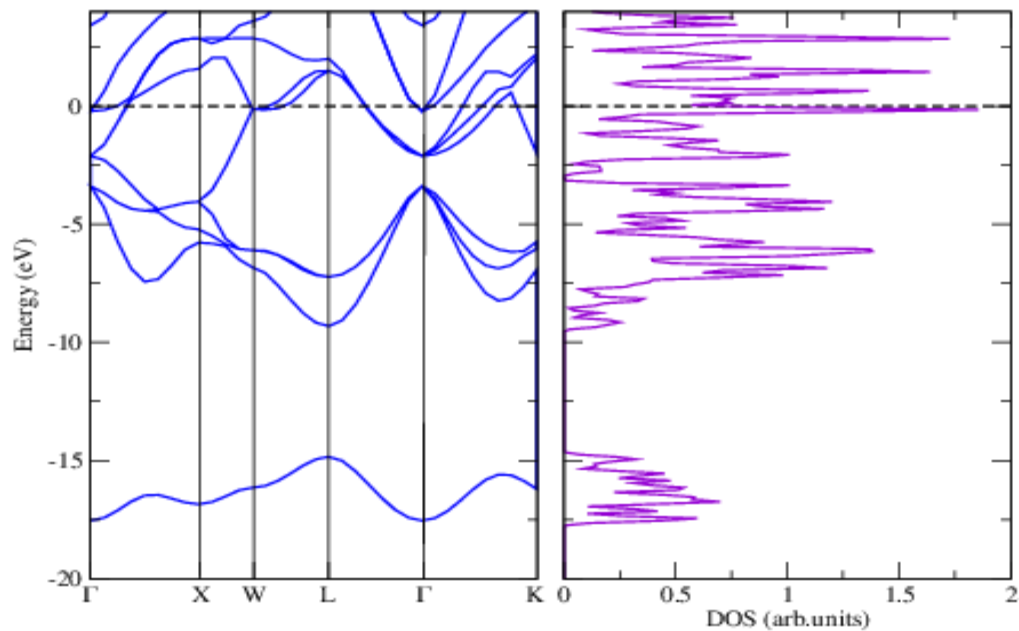
Fig: 5.21a Band structures and DOS for b1
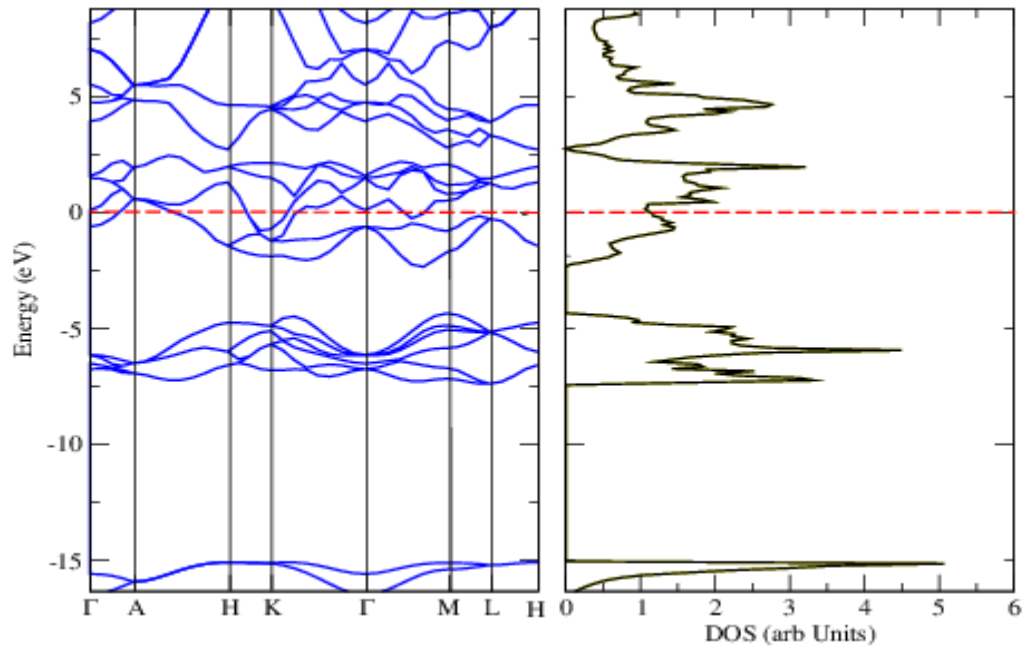
Fig: 5.21b Band structures and DOS for b4
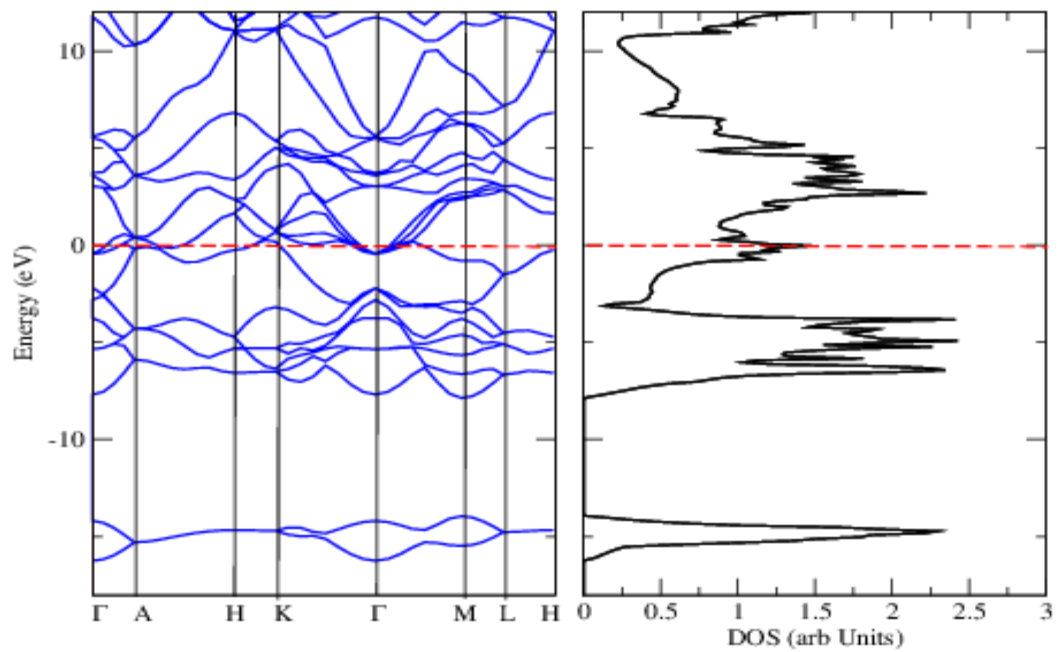
Fig: 5.21c Band structures and DOS for b81
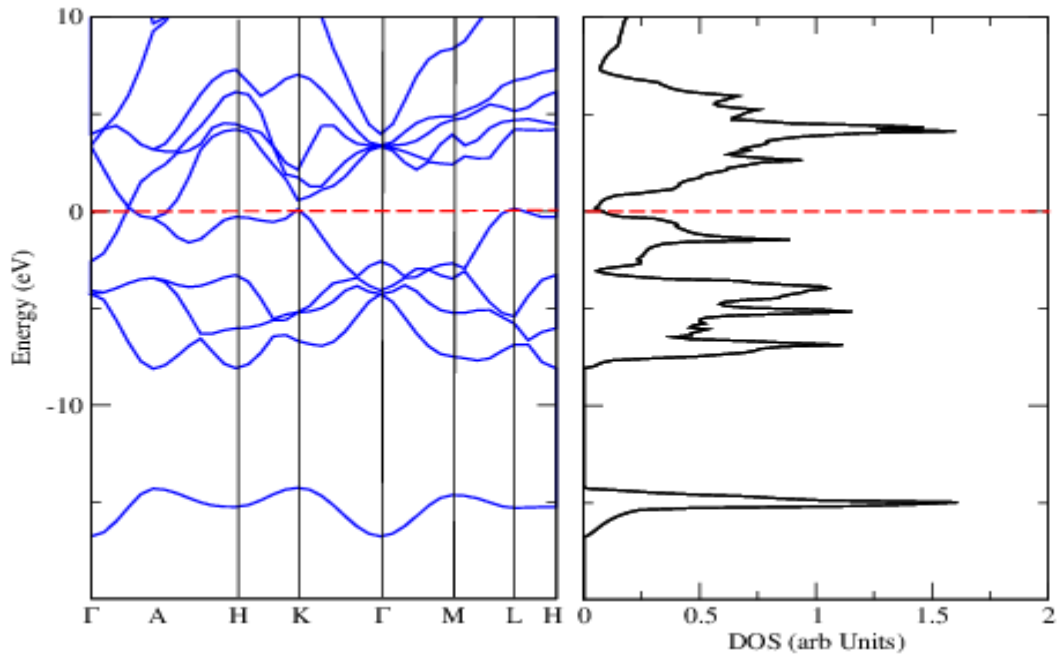
Fig: 5.21d Band structures and DOS for bh

The fig 5.22a to 5.22d of charge density maps corresponds to NbN polymorphs; b1 rocksalt, b4 wurtzite, b81 NiAs and bh WC-type. Looking at the individual elements that make up NbN, Nb has a valence of 13 and N has 5. Therefore Nb has more charge density states than N. This is clearly seen from the maps with Nb atoms having more contours around them than N. For b1 and b4 that have 2 atoms per unit cell, their maps present a dark spot (N atom) that is surrounded by bright patches with many contours (Nb atom) directed towards N vacancy sites (Ethridge *et al.*, 1995), indicating Nb-N bonding in the cubic and hexagonal structures is covalent. On the other hand, b81 and bh with 4 atoms per unit cell present dark contoured patch (Nb atom) with two or no bright spot (N atom). In this case the maps present Nb-Nb metallic bonds indicating hexagonal hybridization where more d states take part in bonding lowering the total energy (Holec *et al.*, 2010). This is a sign that superconductivity in b81 and bh structures is a d-wave with the most favourable

45

structure being b81 which has the lowest energy. Where bright spots are seen, one of the Nb pulls the N forming covalent bond Nb-N. The bonding in the last two is affected by the pseudogap that is seen at the below the Fermi level in b81 and at the Fermi level of bh separating bonding and anti-bonding states.

## 5.2.2 Determined charge density maps
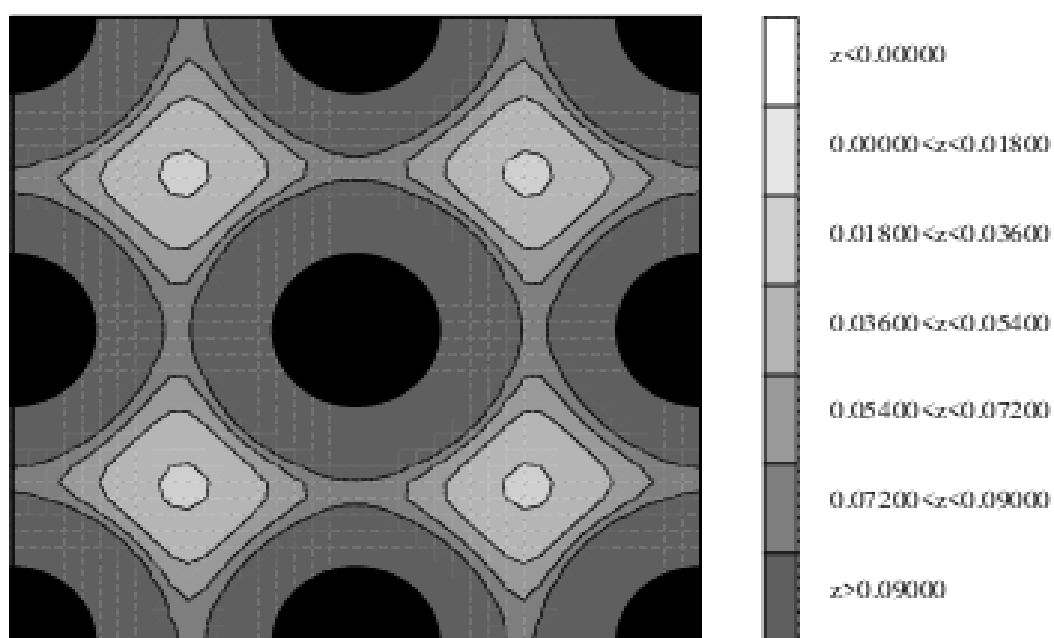
Fig: 5.22a Charge Density for b1
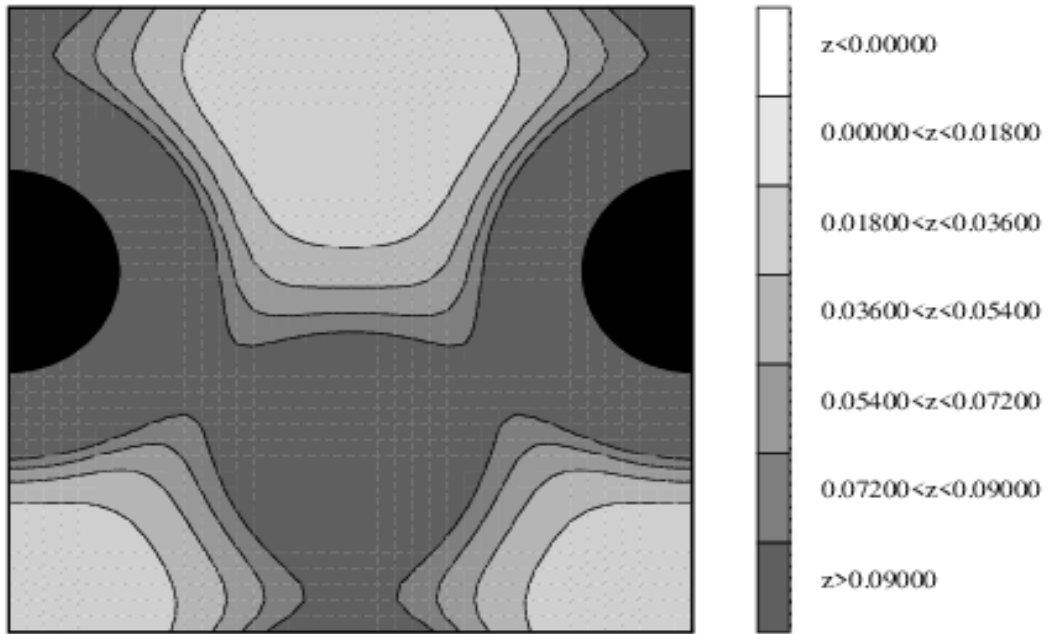
Fig: 5.22b Charge Density for b4
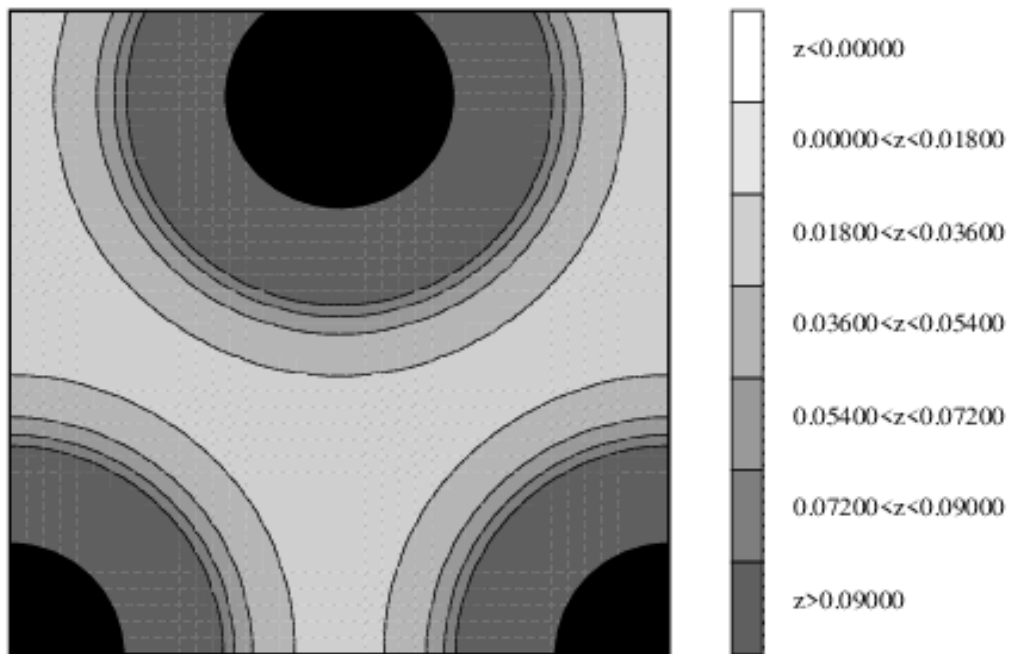
Fig: 5.22c Charge Density for b81
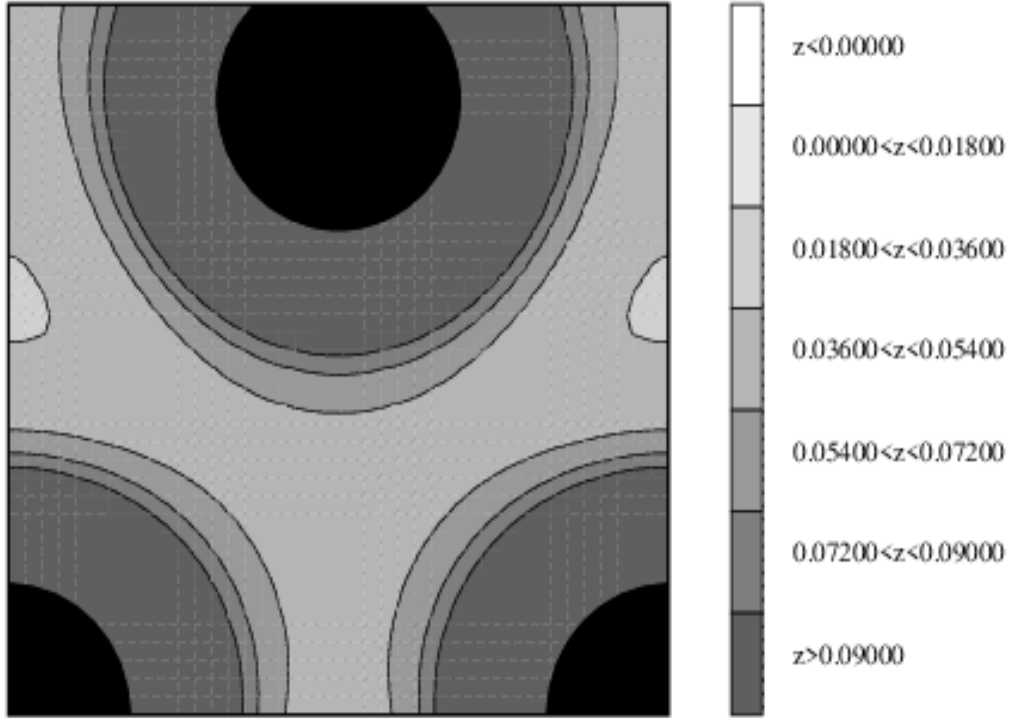
Fig: 5.22d Charge Density for bh

According to (Zou *et al*., 2016) the DOS has a direct consequence in superconductivity. From the graphs of DOS, a pseudogap is observed at the Fermi level of bh and above/below the Fermi level of b4 and b81 respectively. This results to strong hybridizations among the Nb *4d* and N *2p* orbitals causing covalent/ionic bonding. The pseudogap is also referred to as energy gap that appears on either side of a superconductors Fermi level and it is an important factor in superconductivity (Munasia *et al*., 2019). The decrease of density of states at the Fermi level (at the dip "pseudogap") decreases the electron-electron repulsive interaction parameter μ* (coulomb pseudopotential) which is strongly related to the superconducting

transition temperature Tc (Zou et al., 2015). The μ* is equivalent to $\dfrac{0.26N(E_F)}{1+N(E_F)}$

where, N(E_F) is the density at the Fermi level. The μ* is then substituted in the McMillan formula to compute Tc. This means that the larger the pseudogap (the smaller the DOS at Fermi level), the smaller the electron-electron interaction

48

parameter μ* and the higher the Tc. While the smaller the pseudogap (the higher the DOS at Fermi level) the higher the electron-electron interaction parameter μ* and the lower the Tc. Since DOS graphs display a high density at the Fermi level in b4 followed by b81, b1 then bh, therefore, bh stands out as the best among the four for superconductivity applications.

5.3 Determined Magnetic property of Niobium Nitride polymorphs for superconductivity applications.

According to figures 5.31-5.34, the magnetic moment of all the polymorphs are found to be zero, since the sum of spin up and spin down of electrons in their states is zero indicating that the polymorphs are (diamagnetic) non-magnetic. According to table:5.2 below It's clear that b81 and bh have the least range of energy for their DOS.

Table: 5.2 DOS and Energy range

NbN	DOS Range (arb Units)	Energy Range (eV)
b1	-2.0 – 2.0	3.0 – 25.0
b4	-6.0 – 6.0	0 – 25.0
b81	-2.5 - 2.5	2.0 – 30.0
bh	-2.0 – 2.0	4.0 – 30.0

According to (Marouchkine, 2004) a superconductor reveals diamagnetism with total magnetic moment of zero inside the material. The diamagnetism helps the material to expel out magnetic fields from within when it attains temperatures below T_c by developing a dc current on its surface that gives rise to a magnetic field that cancels the external magnetic fields. This is what is referred to as Meissner effect. Meissner effect is what reveals levitation, an effect exhibited by a superconductor

where a magnet is able to float on a superconductor. This happens because in superconductivity state the material is able to expel all the magnetic flux applied to it causing the magnet to float. As stated by (Antoricik *et al.*, 2019), a plot of total and summed Density of States vs energy for Y_2BaCuO_5 revealed diamagnetism in the superconductor. They furthermore, pointed out that it is possible for a metal to become a superconductor in its non-magnetic (zero magnetic moment) state at a suitably low temperature (Transition temperature T_c) also supported by (Shimizu *et al.*, 2001). Therefore, in reference to the above results, the four polymorphs of NbN have good indicators of being superconductors since they are diamagnetic. But b1 and b4 stands out with least range of energy for DOS at 3 to 25 eV and 0 to 25 eV respectively.
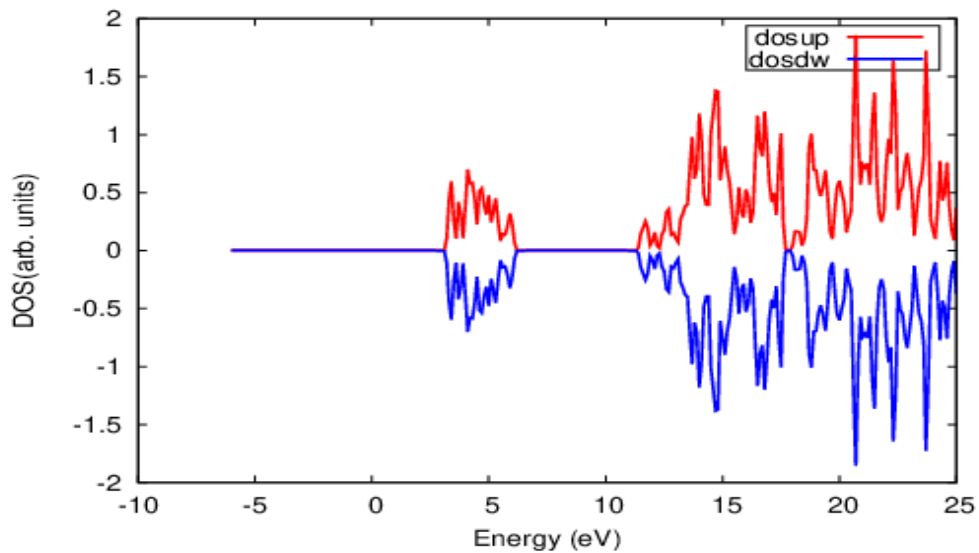
Fig: 5.31 A graph of b1 summed spin up and down of electrons in their states
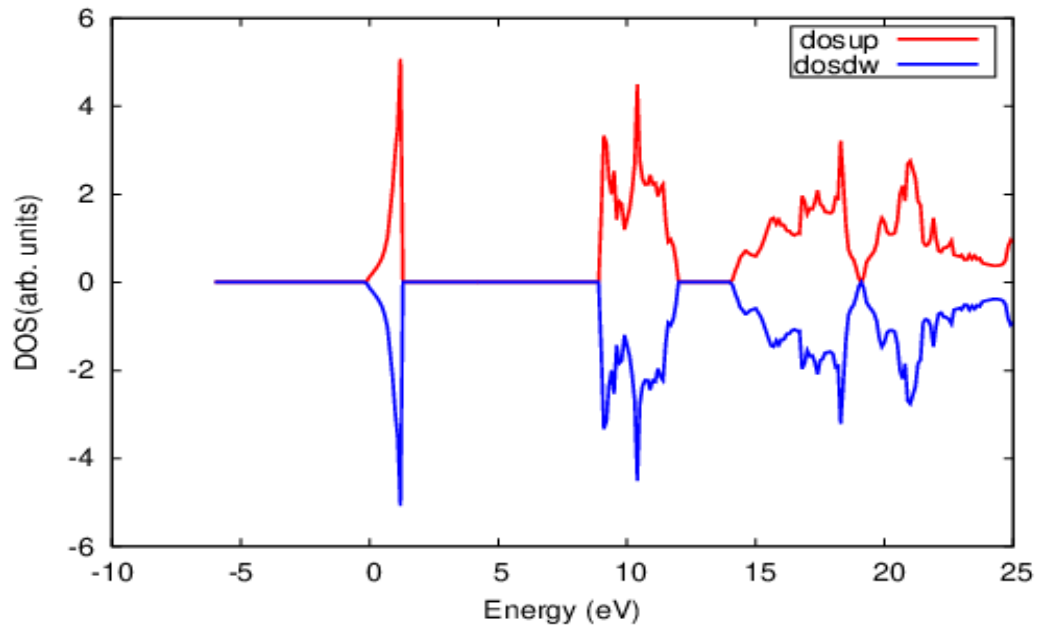
Fig: 5.32 A graph of b4 summed spin up and down of electrons in their states
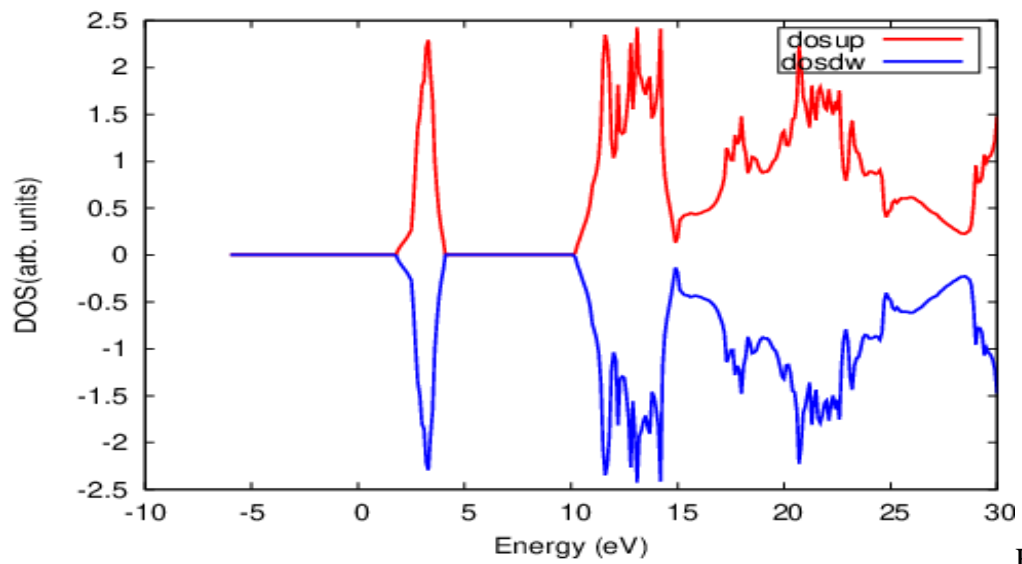
Fig:

5.33 A graph of b81 summed spin up and down of electrons in their states
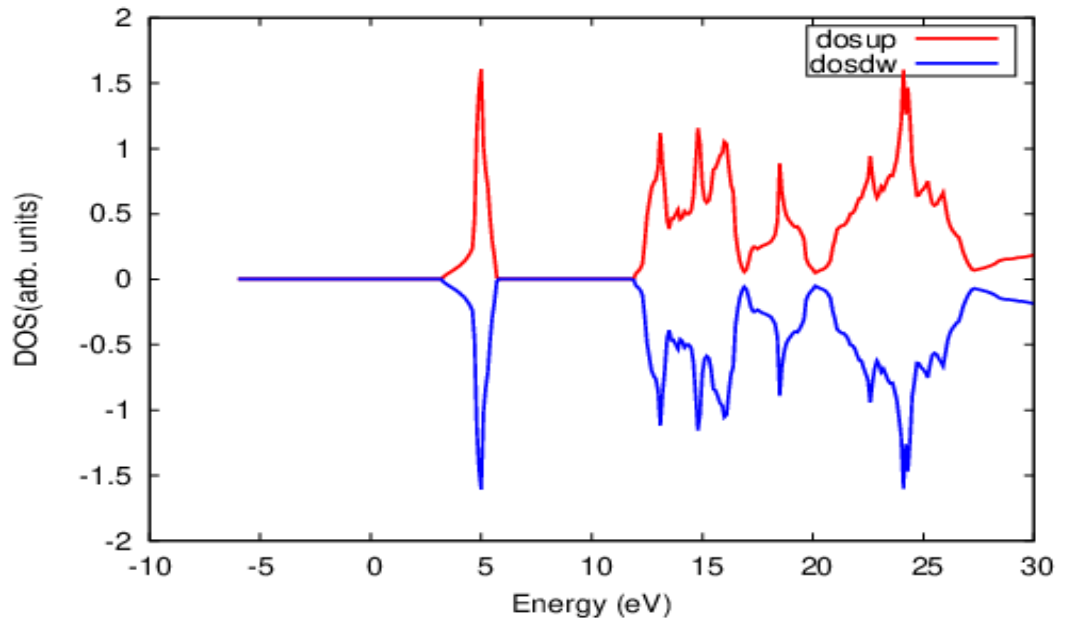
Fig: 5.34 A graph of bh summed spin up and down of electrons in their states

CHAPTER SIX

CONCLUSIONS AND RECOMMENDATIONS

6.1 Conclusions

Under the structural property, the four polymorphs of NbN had negative enthalpies meaning they are easily synthesized at ambient conditions. Among the four polymorphs, b81 turned out to be most stable structure with the least total energy and enthalpy of formation.

According to the electronic property, the four polymorphs were found to be metallic and good conductors of electricity due to non-zero density of states at the Fermi level. Among the four polymorphs bh had the least DOS at the Fermi level.

The four polymorphs were found to be diamagnetic at zero K which helps in electron-electron pairing enhancing superconductivity. The b1 had superior qualities with the least range of energy for DOS.

Overall, bh stands out as the best for superconductivity application, since it has the least DOS at the Fermi level, it is second best in structural and magnetic property.

6.2 Recommendations

The structures were optimized using LDA and Murnaghan equation of state under Quantum Espresso. An extension to this work could be done using other improved exchange correlation functional.

The band structures, DOS and charge density maps were optimized by LDA. An improved functional or LDA+U can be engaged for improvement of the results realized here. Also, the properties can optimized with variation of pressure to ascertain any change.

The magnetic property was based on optimized summed up spin up and down of the electrons in their states. To better this work, the compound could be looked at by singling out the contributions of each element electrons spins to the magnetic property and also using higher exchange correlation functional

REFFERENCES

Ahmed R., (2015). *First Principle Simulations of electrochemical interfaces-a DFT Study*. Kongens Lyngby: Technical University of Denmark.

Antoricik F., Sedmidubsky D., Jirickoova A., Lojka M., Hlasek T., Ruzicka K. and Jankovsky O. (2019). Thermodynamic Properties of Stoichiometric Non-Superconducting phase Y_2BaCuO_5. *Materials* 12:1-11

Babu R. K. and Guo G. Y., (2019).Electron-Phonon Coupling Superconductivity and non-trivial band topology in NbN polytypes.*Physical Review* 1808:1-13

Benvenuti C., Chiggiato P., Parrini L. and Russo R., (1993). Reactive diffusion produced niobium nitride films for superconducting cavity applications. *Elsevier, NuclearInstruments and Methods A* 336: 16-22

Born M. and Oppenheimer J. M., (1927). Quantum Theory of the Molecules.*Annalen der physik*. 457: 84-86

Bull C. L., Mcmillan P. F., Soignard E. and Leinenweber K., (2004). Determination Of the crystal structure of δ-MoN by neutron diffraction.*Journal of Solid state chemistry*. 177:1488-1492

Ceperly D. M. and Alder B.J., (1980).Ground State of the Electron Gas by Astochastic Method.*Physical Review.letters* 45:566-569

Chen X. J., Struzhkin V. V., Wu Z., Cohen R. E., Kung S., Mao H. k. and Hemley R. R.,   (2005). Electric Stiffness of a Superconducting Niobium Nitride Single Crystal Under Pressure. *Physical Review*. B72: 094514-1- 094514-5.

Drozdov A.P., Kong P. P., Minkov V. S., Besedin S. P., Kuzovnikov M. A., Mozaffari S., Balicas L., Balakirev F. F., Graf D. E., Prakapenka V. B., Greenberg E., Knyazev D. A., Tkaz M. and Emerets M. I., (2019).

Superconductivity at 250K in Lanthnum Hydride under high pressures.*Nature 569*, 528-531

Eberhard Engel and Reiner M. Dreizler, (2011).*Density Functional Theory: An Advancedcourse*. Springer-Verlag Berlin Heidelberg. Springer Science and Business Media

Errea I., Calandra M., Pickard C. J., Nelson J., Needs R. J., Li Y., Liu H., Zhang Y., Ma Y. and Mauri F., (2015). Hydrogen Sulphide at High Pressure: a Strongly-anharmonic Phonon-Mediated Superconductor. *Physical Review*. B 114 :157004-157009

Ethridge E. C., Erwin S. C. and Pickett W. E., (1995). Nb_4N_3:Polymorphism in crystalline niobium nitrides. *Physical Review*. B 53:12563-12565

Giannozzi P., Baroni S., Bonini N., Calandra M., Ceresoli D., Chiarotti G. L., Cococcioni M., Dabo I., Corso D.A., Fabris S., Fratesi G., Gebauer R., Gerstmann u., Gougousis C., Kokalj A., Lazzeri M., Martin-Samos L., Marzari N., Mauri F., Mazzarello R., Paolini S., Pasquarello A., Paulatto L., Sbraccia C., Scandolo S., Sclauzero G., Seitsonen A.P., Smogunov A., Umari P. and Wentzcovitch R. M. M., (2009). QUANTUM ESPRESSO: a molecular and Open-source Software project for quantum Simulations of materials. *Journal of physics condensed matter*. 21:1-19

Heil C., Cataldo s., Bachelet B.G. and Boeri L., (2019).Superconductivity in Sodalite-like Yttrium Hydride clathrates.*Physical   ReviewB 99*:220502-220508

Hellman A. and Wang B., (2017). First Principle view of photoelectron-chemistry;water: Splitting as case study. *Inorganics* 2017:1-27

Hohenberg P. and Kohn W., (1964).Inhomogeneous Electron gas.*Physical*

Review 3 B: 136

Holec D., Franz R., mayrhofer H.P. and Mitterer C., (2010).Structure and stability of phases within the NbN-AIN system.*Journal ofPhysics Department of Applied Physics* 43: 1-8

Hutter J., Luthi H. and Parrinello, (2010). Electronic Structure Optimization in Plane-Wave-based density functional calculations by direct inversion in the iterative subspace. *Computational Matter Science*. 244: 1-2

Ivashchenko V., Turchi P.E. and Olifan E.. (2010). Phase stability and mechanical properties of niobium nitrides. *Physical review* B 82:1-9

Jain A., Ong S. P., Hauntier G., Chen W., Richards W. D., Dacek S., Cholia S., Cunter D., D., Skinner D., Ceder G. and Persson K. A., (2013). The Materials Project: A genome approach to accelerating materials innovation. APL materials 1:1-12

Jhi S. H., Ihm J., Louie S. G. and Cohen M. L., (1999). Electronic mechanism of hardness enhancement in transition-metal carbonitrides. *Nature*. 399: 132-134

Kress G. and Joubert D., (1999).From Ultrasoft Pseudopotentials to the projector augmented-wave method.*Physical Review*B.59 : 1758-1775

Kasumov A. Yu., Deblock R., Kociak M., Reulet B., Bouchiat H., Khodos I. I., Gorbatov Yu.-B., Volkov V. T., Journet C. and Burghard M., (1999).Supercurrents Through Single-Welled carbon Nanotubes.*Science*. 284: 1508-1511

Kohn W. and Sham L. J., (1965). Self Consistency Equations Including Exchange and Correlation Effects.*Physical Review* A1133-A1138

Levy R. B. and Boudart M., (1973). Platinum-like behaviour of tungsten carbide in

surface catalysis. *Science*. 181:547

Lindgren M., Currie M., Zeng W.-S., Sobolewski R., Cherednichenko S., Voronov B. and Gol'tsman G. N., (1998). Picosecond Response of a superconducting Hot-Electon NbN Photodetector.*Applied Superconductor*. 6:423-428

Martin R. M., (2004). *Electronic Structure: Basic theory and practical methods*. Cambridge: Cambridge University Press.

Meenaatci A. T. A., Rajeswarapalanichamy R. and Iyakutti K., (2013). Electronic structure, Structural stability, Mechanical and Superconducting properties of group VB nitrides: A first principles study. *Solid state science.* 19:36-39

Mohammad Baiuomy S. K., (2016). *Calculation of the Relative Life Time and Optical Properties for Three-Dimensional (3D) Hybrid Perovskites*. University of The Witwatersrand: Johannesburg.

Monkhorst H. and Pack J., (1976). Special points for brillouin-zone intergrations.*Physical Review* 5188: 1-3

Mora G. S., Lopez C. O., Murillo J. F., Moreno-Armenta M. G. and Espitia M. J. (2018), Computational Calculation of Energetic Stability, Electronic Properties and Magnetism in the Alloys $Nb_{1-x}Cr_xN$. *ContemporaryEngineering Sciences* 11: 88

Mourachkine Andrei, (2004). *Room Temperature Superconductors*.Meadow walk, Great Abington, Cambridge, UK. Cambridge International Science Publishing

Munasia E., Rapando B. W. and Ndinya B., (2019). Superconducting Parameters of Cuprates Due to Microwave Irradiation in The Framework of The Variational Theory. *Journal of Multidisciplinary Engineering Science and Technology 6*:10927-10932

Murnaghan F. D., (1944). The Compressibility of Media Under Extreme Pressure. *NationalAcademy of Science of the United States of America* 30:1-5

Perdew J. P., (1985). Density functional theory and the band gap problem. *InternationalJournal of Quantum Chemistry*

Perdew J. P. and Zunger A., (1981), Self-interaction correction to density-functional approximations for many-electron systems.*Physical Review* B23:5048-5079

Phillips J. and Kleinman L., (1959). New Methods for Calculating wave functions in crystal and molecules. *Physical Review* 287:287-294

Rapando B. W., Tonui J. K., Khanna K. M. and Mang'are P. A., (2016). The Diagonalised *t-J* Hamiltonian and the Thermodynamic Properties of High-T_c Superconductors.*American Research Journal of Physics* 2016: 1-11

Rapando B. W., Khanna K. M., Tonui J. K., Sakwa T. W., Muguro K. M., Kibe H., Ayodo Y. K. and Sarai A., (2014). The Dipole Mediated t-J Model For High-T_c Superconductivity. *International Journal of physics and Mathematical sciences*5: 33-37

Rinke P., Qteish A., Neugebauer J., Freysoldt C. and Scheffler M., (2005). Combining Gw calculations with exact-exchange density functional theory: an analysis of valance-band photoemission for compound semiconductors. *New Journal of physics* 126:1-35

Setyawan W. and Curtarolo S., (2010). High-throughput electronic band structure calculations: challenges and tools. *Computational Materials Science* 49: 2

Shimizu K., Kimura T., Furomoto S., Takeda K., Kontani K., Onuki Y. and Amaya K., (2001). Superconductivity in the non-magnetic state of iron under pressure.*Nature vol* 412:316-318

Sholl D. S. and Steckel J. A., (2009).*Density Functional Theory: a practical Introduction*. New Jersey: John Wiley and Sons. Inc. Hoboken.

Soignard E., Shebanova O. and Mcmillan P. F., (2007). Compressibility Measurements and Phonon Spectra of hexagonal transition-metal nitrides at high pressure: ε-TaN, δ-MoN and Cr_2N. *Physical Review*. B 75:014104-0141013

Somayazulu M., Ahart M., Mishra A. K., Gaballe Z, M., Baldini M., Meng Y., Struzhkin V.V. and Hemley R. J., (2019).Evidence for superconductivity above 260K in Lanthanum Superhydride at Megabar pressure.*PhysicalReview* 122: 027001-1 – 027001-6

Stampfl C., Mannstadt W., Asahi R. and Freeman A. J., (2001). Electronic structure and physical properties of early transition metal mononitrides: Density-Functional theory LDA, GGA and Screened-Exchange LDA FLAPW calculations. *Physical Review B* 63:155106-155117.

Syrivastava A., Chauhan M. and Singh R. K., (2011). Pressure induced phase transition in transition metal nitrides: *Ab initio* study. Physics status solidi B 248: 12

Terao N., (1965). Structure Des Nitrures De Niobium. Japanese Journal of Apllied Physics. 4: 353-367.

Tyuterev V. G. and Nathalie V., (2006).Murnaghan's equation of state for the electronic ground state energy.*Elsevier Computational materials science* 38:350

Troullier N. and Martins J. L., (1991).Efficient Pseudopotential for plane-wave Calculation.*Physical Review* B 43:8861-8869

Ulloa R. Z., (2019). Superconductivity and Microwaves, Superconductivity and Superfluidity. doi:https://dx.doi.org/105772/intechopen.86239.

Wang Z. H., Kuang X. Y., Huang X. F., Lu P. and Mao A., (2011). Pressure Induced Structural Transition and thermodynamic Properties of NbN and Effect of Metallic Bonding on its hardness.*The frontiers of physics*. 56002:1-6

Woods N. D., Payne M. C. and Hasnip P. J., (2019).Computing the consistent field in Kohn-Sham density functional theory.*Journal of physics: condensedmatter* 31:45

Wu L., Chen L., Wang H., Wang Q., Wo H., Zhao J., Liu X., Wu X. and Wang Z., (2017). Measurements of Meissner effect in micro-sized Nb and the FeSe crystals using an NbN nano-SQUID. *Superconductor science and technology* 30: 074011.

Zhao E., Wang J., Meng J. and Wu Z., (2010).Structural, Mechanical and electronic Properties of 4d Transition metal Mononitrides by first-principles.*Elsevier* 47:1064-1071

Zou Y., Qi X., Zhang C., Ma S., Zhang W., Li Y., Chen T., Wang X., Chen Z., Welch D., Zhu P., Liu B., Li Q., Cui T. and Li B., (2016). Discovery of Superconductivity in Hard Hexagonal ε-NbN. *Scientific Reports*. 6:1-9

Zou Y., Wang X., Chen T., Li X., Qi X., Welch D., Zhou P., Liu B., Cui T. and Li B., (2015). Hexagonal-Structured ε-NbN: Ultra Incompressibility, High Shear Rigidity, and Possible Hard Superconductivity Material. *Scientific reports*. 3B:1-11

Appendix 1 : Cell dimension for NbN Polymorphs
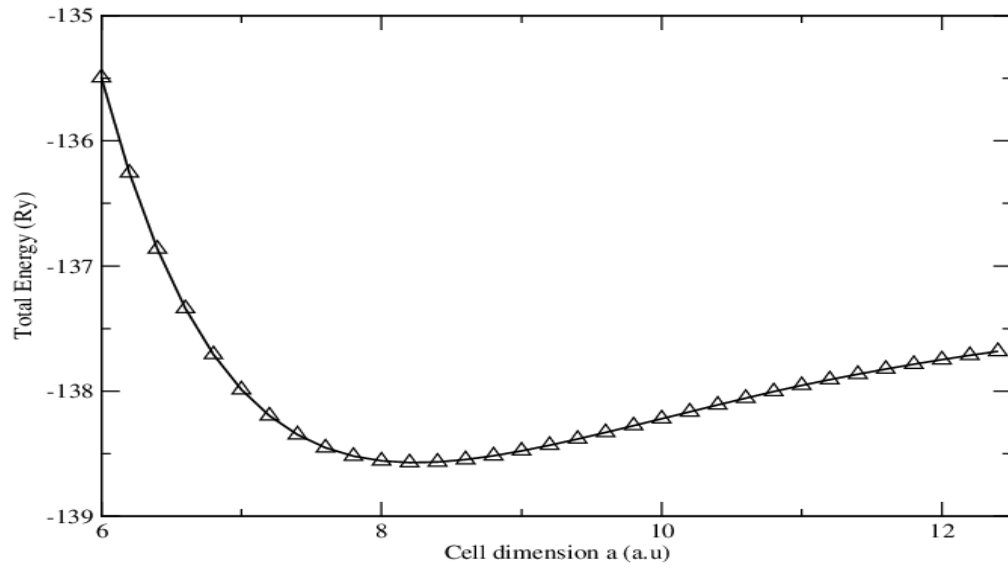
Fig: 6.1a Cell dimension *a* convergence for b1
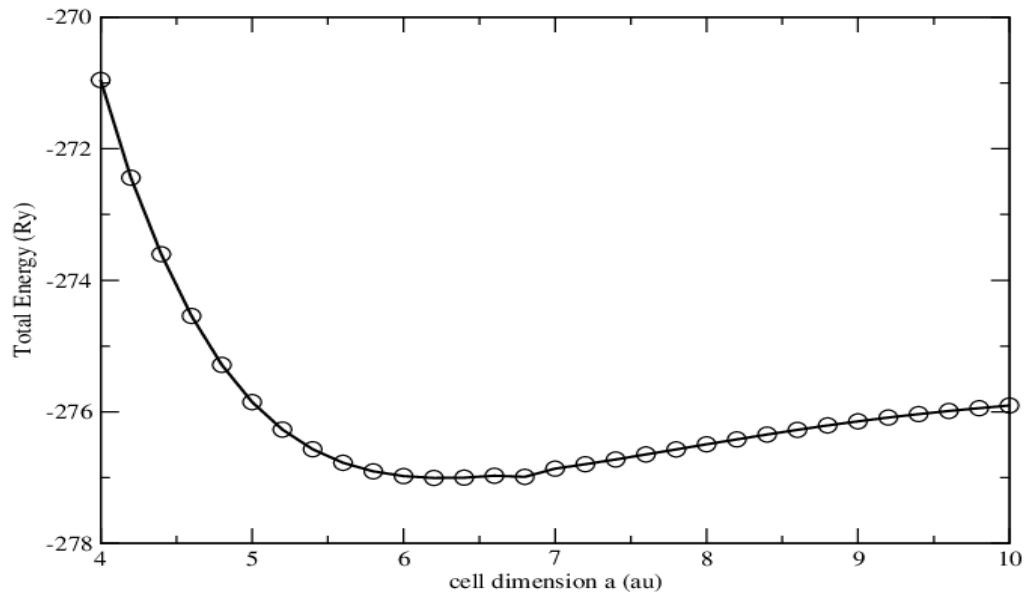

Fig: 6.1b Cell dimension *a* convergence for b4
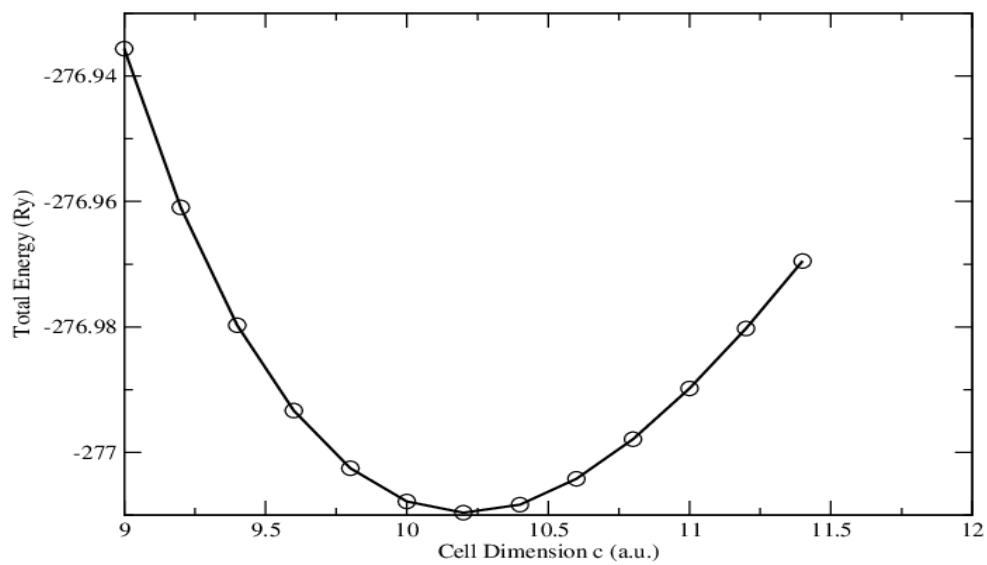
Fig: 6.1c Cell dimension *c* convergence for b4
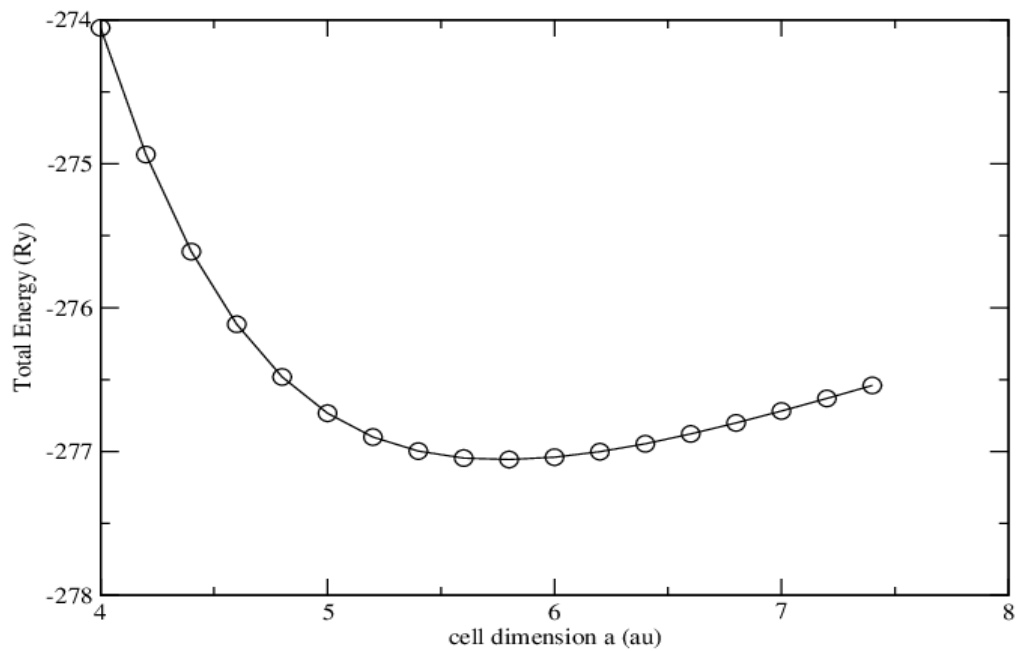
Fig:

6.1d Cell dimension a convergence for b81
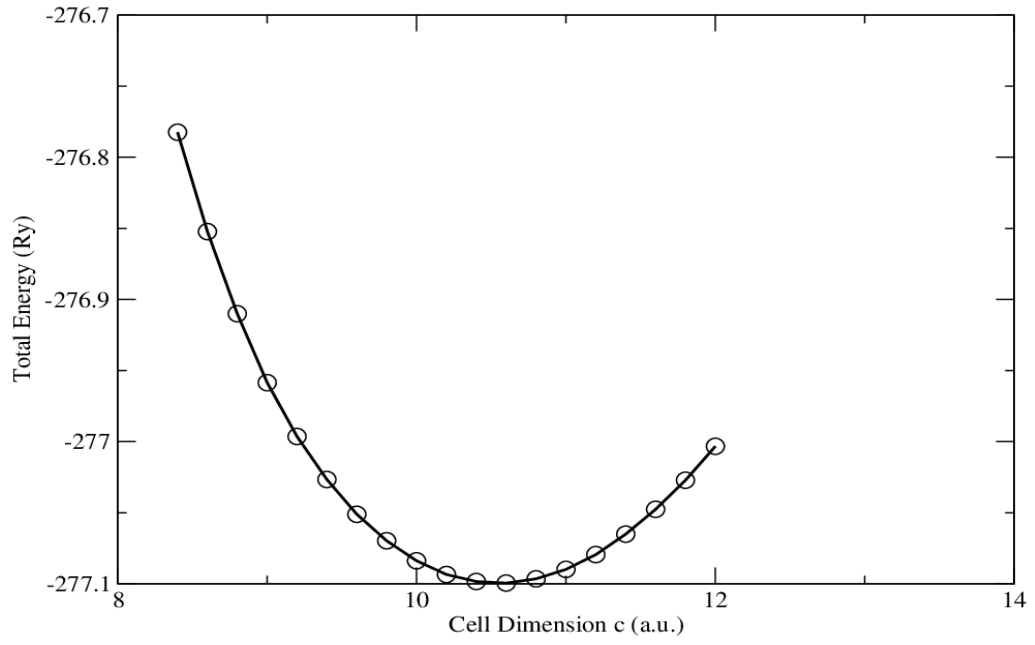
Fig:

6.1e Cell dimension c convergence for b81
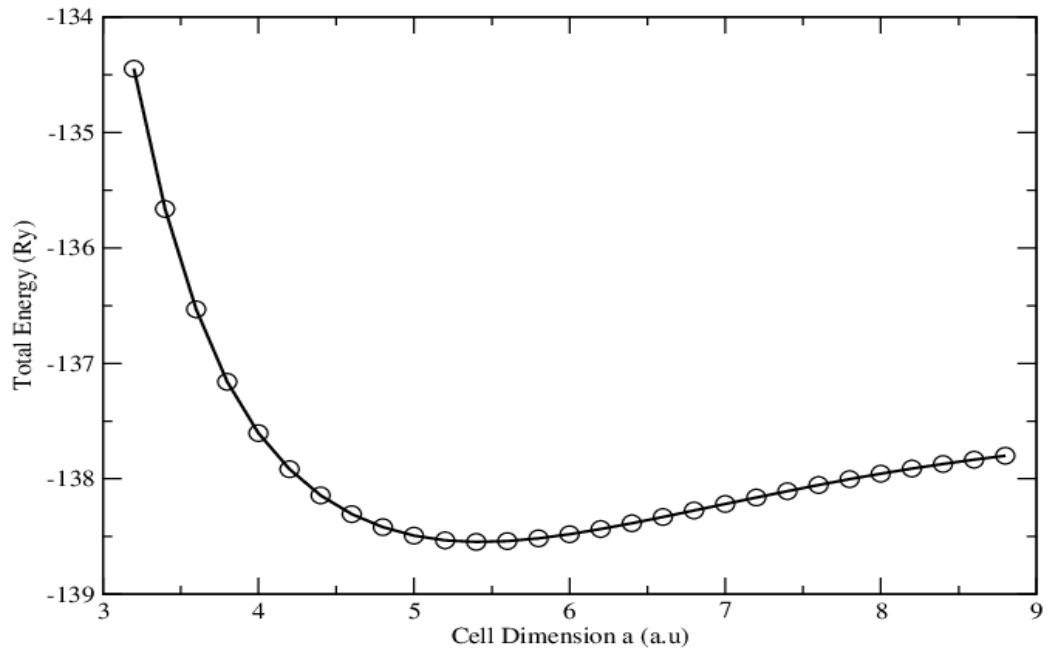
Fig: 6.1f Cell dimension *a* convergence for bh
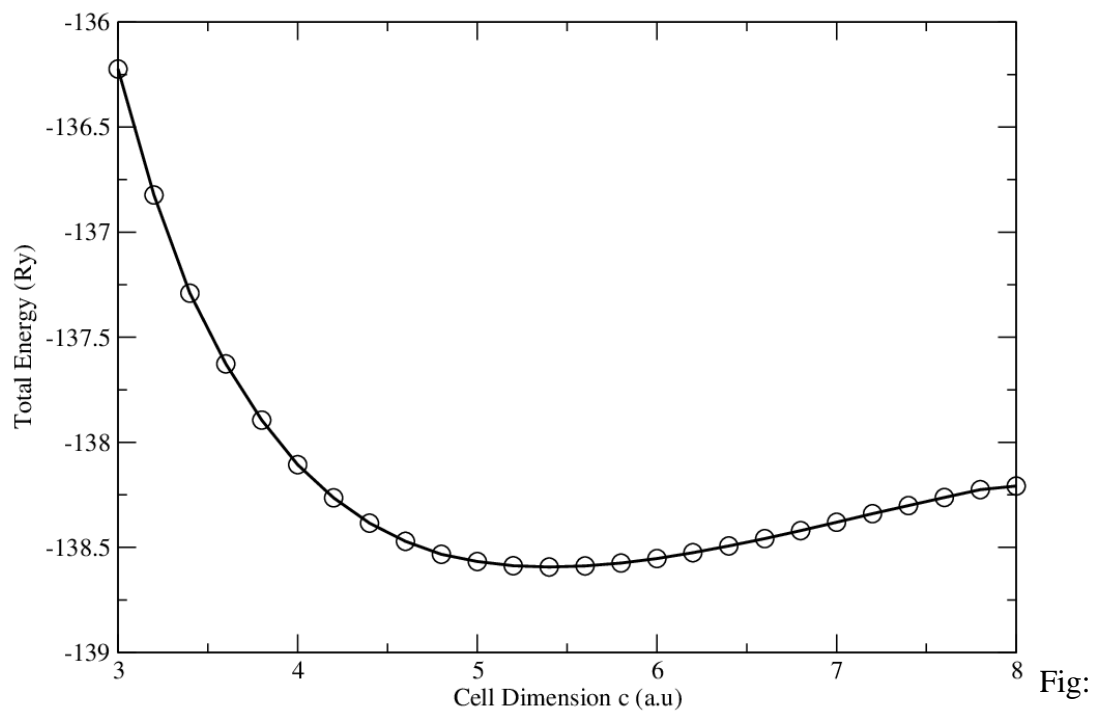
6.1g Cell dimension c convergence for bh

**Appendix 2: k-points graphs for NbN polymorphs**
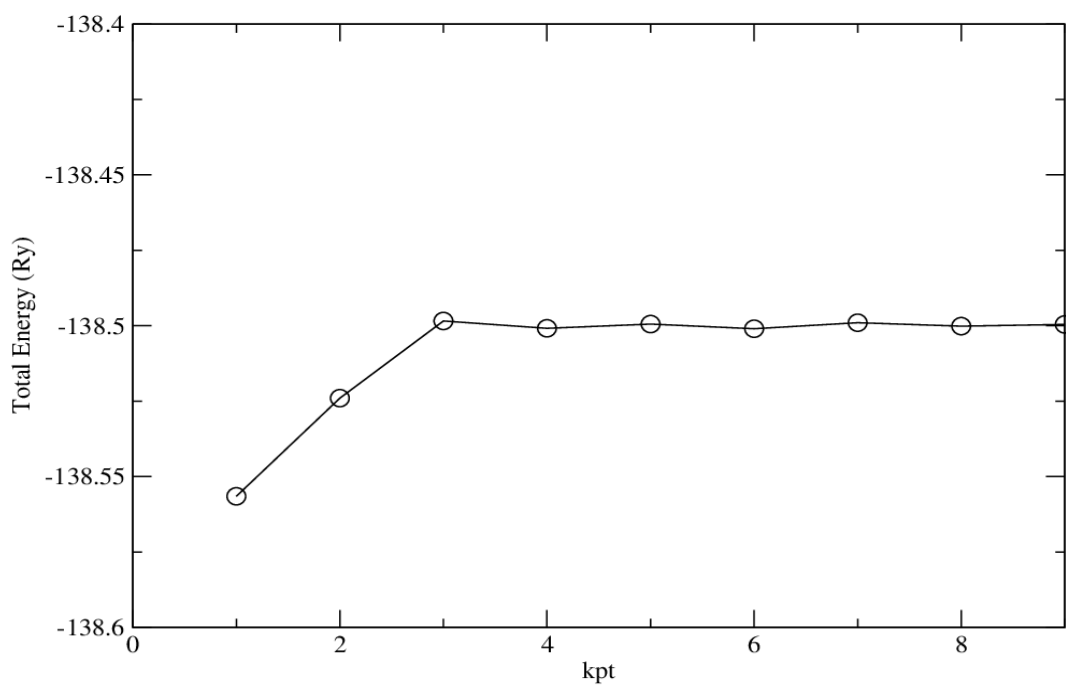
Fig: 6.2a A graph of Total Energy (Ry) vs k-point for b1
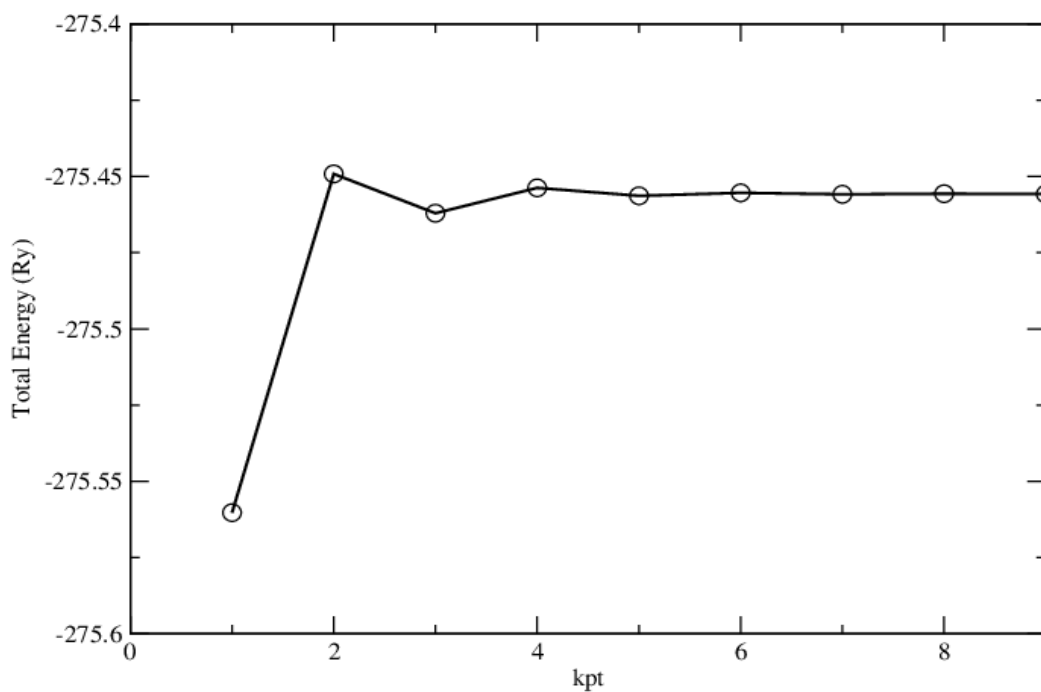
Fig: 6.2b A graph of Total Energy (Ry) vs k-point for b4
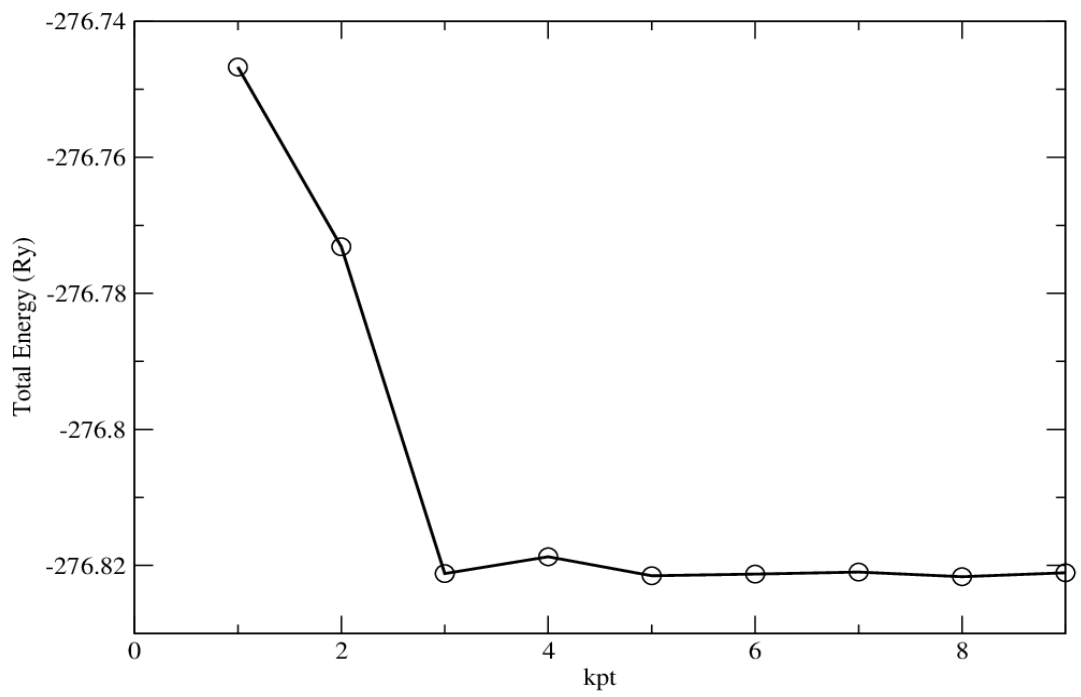
Fig: 6.2c A graph of Total Energy (Ry) vs k-point for b81
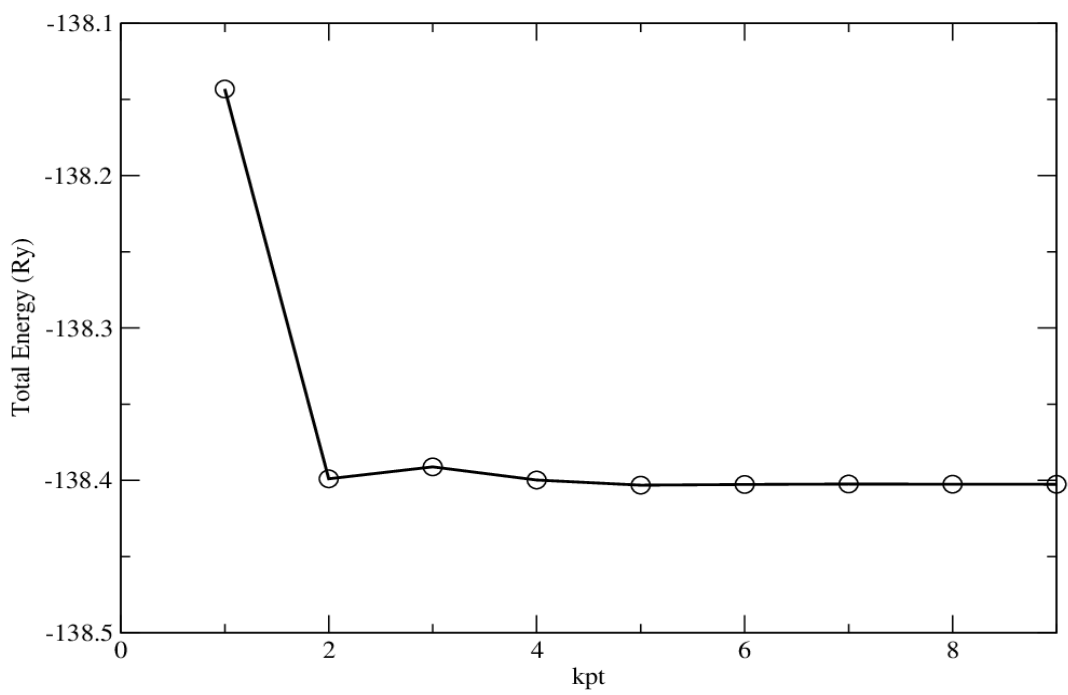
Fig: 6.2d A graph of Total Energy (Ry) vs k-point for bh

Appendix 3: E-cut graphs for NbN polymorphs
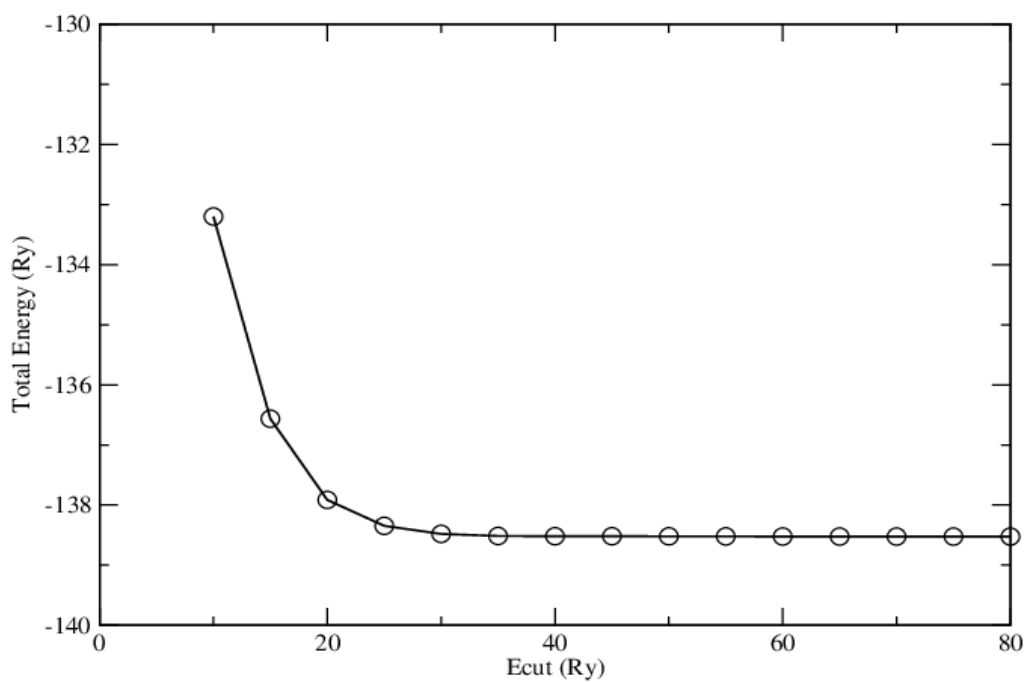
Fig: 6.3a A graph of Total Energy vs E-cut for b1
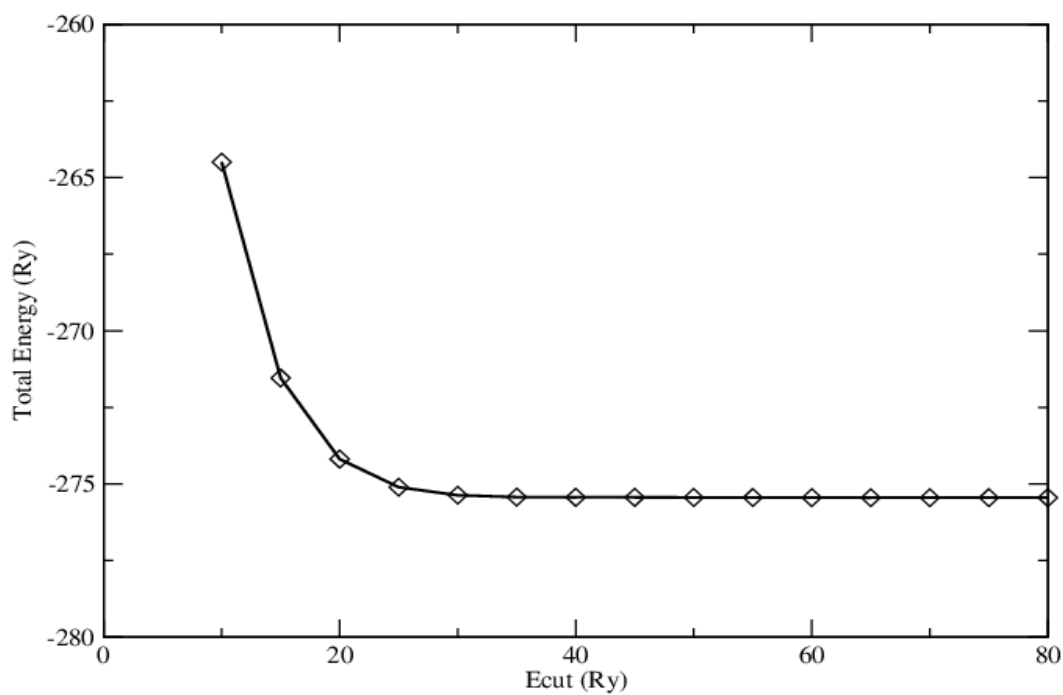
Fig: 6.3b A graph of Total Energy vs E-cut for b4
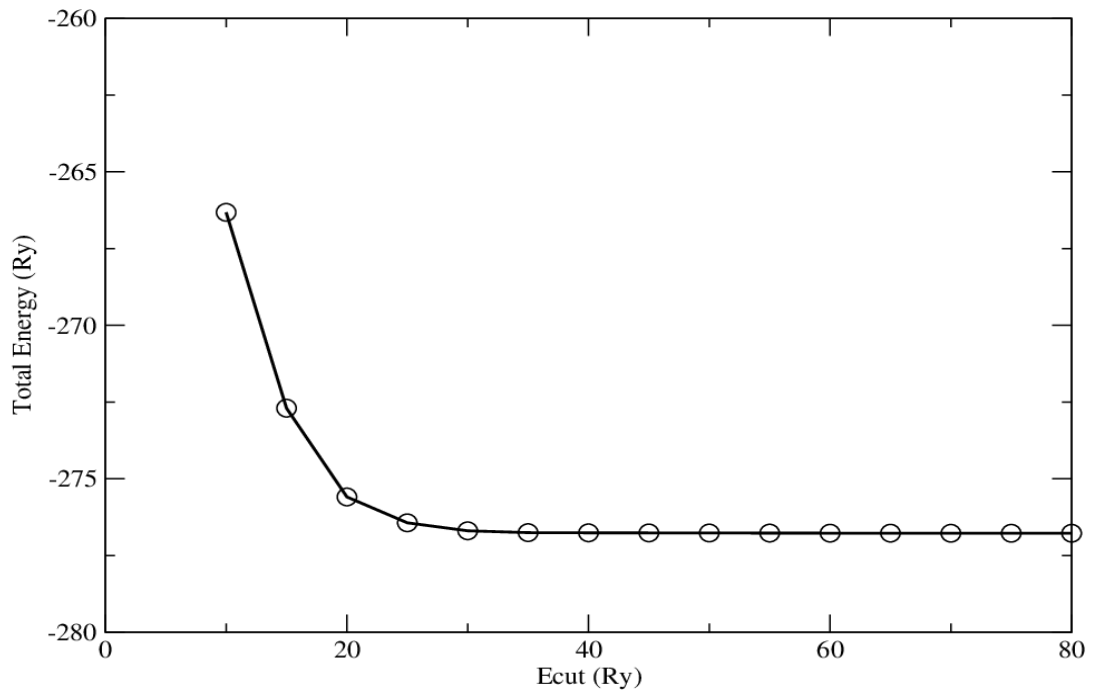
Fig: 6.3c A graph of Total Energy vs E-cut for b81
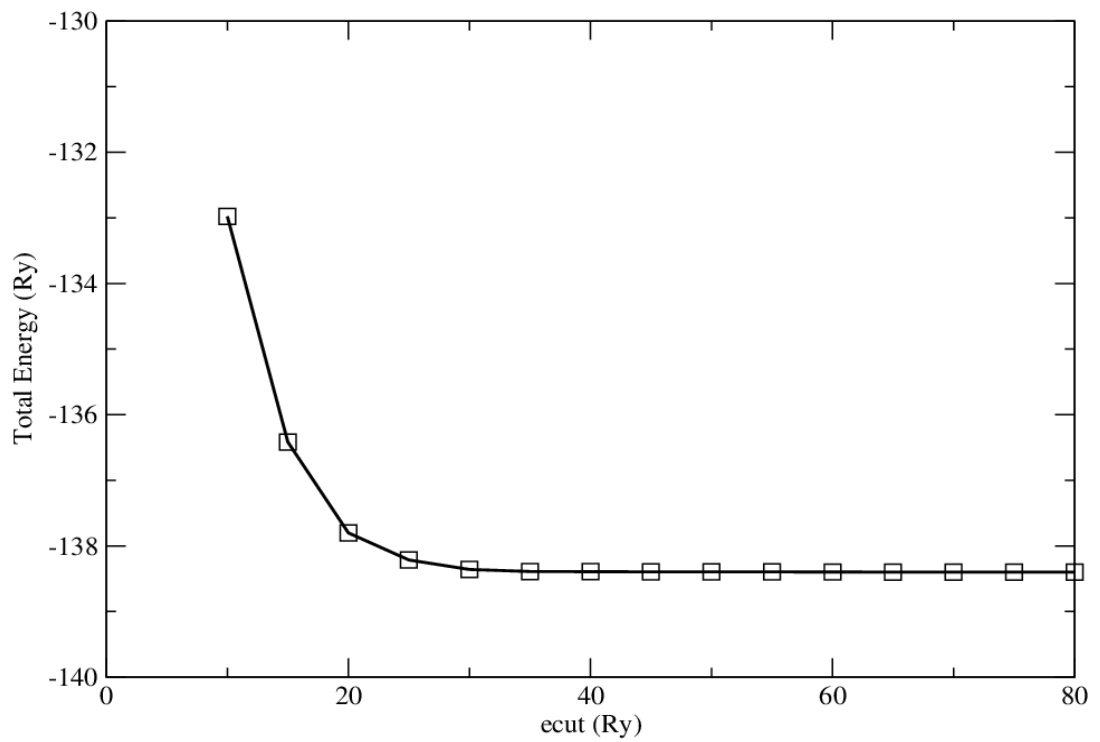
Fig: 6.3d A graph of Total Energy vs E-cut for bh

69

Appendix 4: Publication related to this thesis

1. Isiaho S. L., Rapando B. W. and Otunga H. O., (2020). Structural, Magnetic and Electronic Properties of NbN Polymorphs by *Ab-initio* study. *JMEST* 7:12050-12057